Science of the Total Environment 880 (2023) 163356

Contents lists available at ScienceDirect

Science of the Total Environment

journal homepage: www.elsevier.com/locate/scitotenv

Sinking delta: Quantifying the impacts of saltwater intrusion in the Indus Delta of Pakistan

Hafsa Aeman [a,*], Hong Shu [a], Sawaid Abbas [b,c], Hamera Aisha [d], Muhammad Usman [b]

[a] State Key Laboratory of Information Engineering in Surveying, Mapping and Remote Sensing, Wuhan University, China
[b] Smart Sensing for Climate and Development, Center for Geographical Information System, University of the Punjab, Lahore 54590, Pakistan
[c] Department of Land Surveying and Geo-Informatics, The Hong Kong Polytechnic University, Hong Kong
[d] World Wide Fund for Nature - Pakistan (WWF-Pakistan), Pakistan

HIGHLIGHTS

- The study evaluates the changes in the shoreline of the Indus delta, which has been shrinking, through the integration of a multispectral statistical approach.
- Spatial data on coastal erosion from this study is critical for planners and decision-makers to develop effective strategies, and adapt to mitigate erosion.
- The study calculates coastal erosion and accretion using the tasselled cap transformation and linear regression rates also observed an impact on mangroves due to intruding salinity.
- Findings indicate the erosion rates in the Western Delta are exceptionally high, followed by Middle West and Middle East delta.
- The study spurs discussions on future Coastal Zone Management plans and methodologies for Integrated Coastal Zone Management framework.

GRAPHICAL ABSTRACT

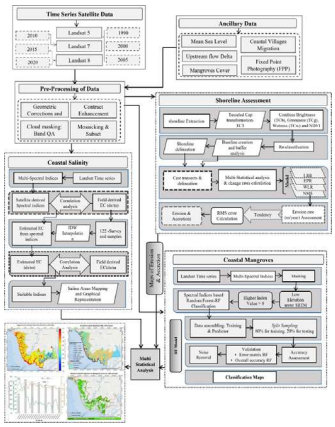

ARTICLE INFO

Editor: Fernando A.L. Pacheco

Keywords:
Indus Delta
Erosion
Accretion
Salinity
Climate change
Landsat
Mangroves cover change

ABSTRACT

This study focused on an integrated assessment of coastline change and its impacts on the deltaic sustainability of the Indus Delta, the world's fifth-largest delta. The increase in salinity and degradation of mangrove habitat was examined using multi-temporal Landsat satellite imagery from 1990 to 2020. The tasselled cap transformation indices, multi-statistical End Point Rate and Linear Regression were used to extract the shorelines rates. Mangrove cover area was estimated by applying the Random Forest clasification approach. Impacts of coastal erosion on mangroves and sea-water salinity were determined through the association between electrical conductivity and vegetation soil salinity index (VSSI). The accuracy of the analysis was evaluated using ground truth information obtained from field surveys and Fixed-Point Photography. Major findings of the analysis indicate that the North-West Karachi experienced accretion at an average rate of 7.28 ± 1.15 m/year, with medium salinity (VSSI<0.81) and increased mangrove cover, from 11.0 km^2 area in 1990 to 14.5 km^2 in 2020. However, the Western Delta has undergone massive erosion at a mean rate of −10.09 ± 1.61 m/year with obtrusive salinity (0.7 ≤ VSSI ≤ 1.2) and 70 km^2 of mangrove cover loss. In the Middle West Delta and Middle East Delta erosion is observed at an average rate of −28.45 ± 0.55 m/year rate, with high

* Corresponding author.
E-mail address: hafsa.aeman@whu.edu.cn (H. Aeman).

http://dx.doi.org/10.1016/j.scitotenv.2023.163356
Received 13 January 2023; Received in revised form 3 April 2023; Accepted 3 April 2023
Available online 6 April 2023

obtrusive salinity (0.43 ≤ VSSI ≥ 1.32) and rapid mangroves cover loss (14 km^2). The Eastern Delta was relatively stable and accelerating towards the sea with increasing mangrove cover (629 km^2). Our analysis revealed that erosion, which occured due to reduced sediments flow linked to development of water infrastructures as well as climate change, have serious implications for the ecosystem. Future policy and action-plans should priotitise addressing vulnerabilities by integrate nature-based solutions for revival of the Delta.

1. Introduction

The coastal intrusion contributes to the increased vulnerability of local communities and degrades mangroves and associated ecosystem services in Pakistan. Pakistan is listed among the top ten countries in the world vulnerable to the impacts of climate change and its coastline is adversely affected in the form of sea level rise and coastal intrusion (Kanwal et al., 2019). The Indus delta is ranked as the third most vulnerable delta facing severe impacts of climate change. Pakistan has lost its mangroves cover at an alarming rate of 2 % per year during the past 100 years (Sanderman et al., 2018) and the coastal intrusion will further accelerate the loss of mangrove cover. The government of Pakistan, civil society organizations and the private sector have been making notable efforts to increase mangroves cover through various afforestation initiatives especially in the province of Sindh (WWF-Pakistan, 2005) These efforts are however limited and need concrete monitoring and long-term concentrated solutions, particularly in the lower parts of the Indus delta which is extremely vulnerable and others remote regions of the country.

The development of dams and barrages upstream Indus River has reduced the flow of freshwater in the Indus Delta, which is also intensifying coastal intrusion. The coastal intrusion is putting the lives and livelihood of over one million inhabitants of the delta at risk, contributing towards the loss of land and degradation of the precious ecosystem and its associated Ecosystem Services (ES) along the coastline of Pakistan. The deltaic regions support over 500 million people in Asia and Africa alone (Amjad et al., 2007; Giosan et al., 2006). These regions however are extremely vulnerable to coastal erosion due to several factors including their physical characteristics, climate change, and rampant sustainable infrastructure development (Genz et al., 2007).

Previously, changes in shorelines position in deltaic regions have been assessed by quantifying change over time by using Geographic Information Systems (GIS) based tools in various regions e.g., Kannyakumari Coastline, India (Suresh and Sundar, 2011), Coastal Ramsar wetlands of Turkey (Kuleli et al., 2011), Konya River Basin, Turkey (Durduran, 2010) and the North Sinai coast, Egypt (Nassar et al., 2019), etc. Many studies have demonstrated high potential in coastline delineation and mapping of geomorphological changes for different shoreline conditions using the GIS approaches in different parts of the world, India (Baig et al., 2020), Bangladesh (Kalivas et al., 2003) and along the coastline areas of Mediterranean Sea (Ghosh et al., 2015; Petropoulos et al., 2015; Saavedra, 2005; Passer et al., 2014). Due to repetitive coverage and synoptic view, extraction of shorelines change using GIS and remote sensing (RS) is very helpful (Pimple et al., 2018). GIS and RS-based methodologies employed a range of tools including image classification techniques (Adarsa et al., 2012), spectral bands rationing (Lira and Taborda, 2014; Sarwar and Woodroffe, 2013), image segmentation (Semenov et al., 1999) and edge detection (Zhang et al., 2013). For example, change detection techniques based on remote sensing were used to assess shoreline delineation in Yellow River, China (Cui and Li, 2011; Ji et al., 2020; Liu et al., 2012). The previous studies (Pimple et al., 2018) also used Random Forest (RF) classifier for mangroves classification in Google Earth Engine (GEE) with 96 % overall accuracy for the years 1987 and 2017, respectively. The primary advantage of using Random Forest is its superior overall classification accuracy compared to other popular algorithms because of its object-based processing property (Eisavi et al., 2015). It also sustains the overall classification error balance with the size of class distribution with little or no manual intervention using data features regulation process design (Zeferino et al., 2020). The approach described can help to sustain the overall classification error balance, allowing for the accurate identification and monitoring of changes in salinity levels and their effects on agricultural land use.

By using this approach, a targeted strategy was previosuly developed to mitigate the impacts of coastal intrusion and climate change on agriculture in vulnerable regions such as third-largest Mekong Delta of Vietnam (Liu et al., 2012; Zhu et al., 2021; Li et al., 2020). Salinity intrusion accelerated by coastline changes is one of the influential factors leading towards land degradation and a significant threat to the sustainable growth of coastal communities' livelihoods (Solangi et al., 2020). Landsat thematic mapper (TM)/enhancement thematic mapper plus (ETM+) data have been used for vulnerability assessment due to soil salinity contamination and monitoring a variety of environmentally associated coastal intrusion problems (Liou et al., 2017; Verma et al., 1994). Seawater intrusion is a significant problem for coastal communities, as it can result in increased salinity levels in freshwater aquifers and negatively impact agriculture and drinking water sources (Parizi et al., 2019). The Indus delta ecosystem is being subjected to significant environmental and social pressures, causing a loss of habitats and biodiversity, a reduction in fish productivity, and social problems for coastal communities (Amjad et al., 2007). Overall, the present study conducted in 2023 revealed that about 88 % of the Indus delta is affected by subsurface seawater intrusion (Solangi et al., 2023). The once-thriving Indus Delta, which covered an area of 1.3 million hectares in 1833, has diminished to just 0.1 million hectares, representing a 92 % decrease in its size (Solangi et al., 2023).

A few studies have focused on mapping coastline degradation on a large scale and its impact on morphological changes (Din Hashmi and Ahmad, 2018; Giosan et al., 2006; Ijaz et al., 2019; Kanwal et al., 2019; Solangi et al., 2019). As seawater intrusion continues to pose a major challenge to delta regions, where rising sea levels and seawater intrusion are causing saltwater to infiltrate freshwater aquifers. Deltas, with their low-lying lands and high water tables, are especially vulnerable to intrusion (Parizi et al., 2019). To mitigate the problem, reducing intrusion and implementing recharge methods are crucial (Cui and Li, 2011). Mangrove forests in Pakistan are facing serious stresses which jeopardize their sustainability (Mukhtar and Hannan, 2012). Effective management of freshwater resources in delta regions is critical for sustainability, yet it has received limited attention in studies. Many small to large-scale studies have been carried out to determine the erosion and accretion along the coastline (Ijaz et al., 2019; Mahboob and Atif, 2016; Siddiqui and Maajid, 2004) without demarcating its systematic impacts on sustainability.

In this study, our primary objective was to comprehensively understand the morphological changes along the entire Indus Delta and to develop a systematic approach to prevent further degradation, leveraging remote sensing observations. Specifically, we sought to address the systematic impacts by using a machine-learning Random Forest approach to determine the time-series dynamics of coastline change. For this purpose, multitemporal Landsat images were utilized to analyze the coastal intrusion dynamics with causative factors such as rising salinity and its impact on the mangrove forest cover. The objective of this study was to spur discussions on future coastal zone management plans and methodologies for establishing an Integrated coastal zone management framework.

2. Materials and methods

2.1. Study area

The coastline of Pakistan stretches about 1000 km, out of which about 320 km lies in Sindh province (Fig. 1). The study includes the

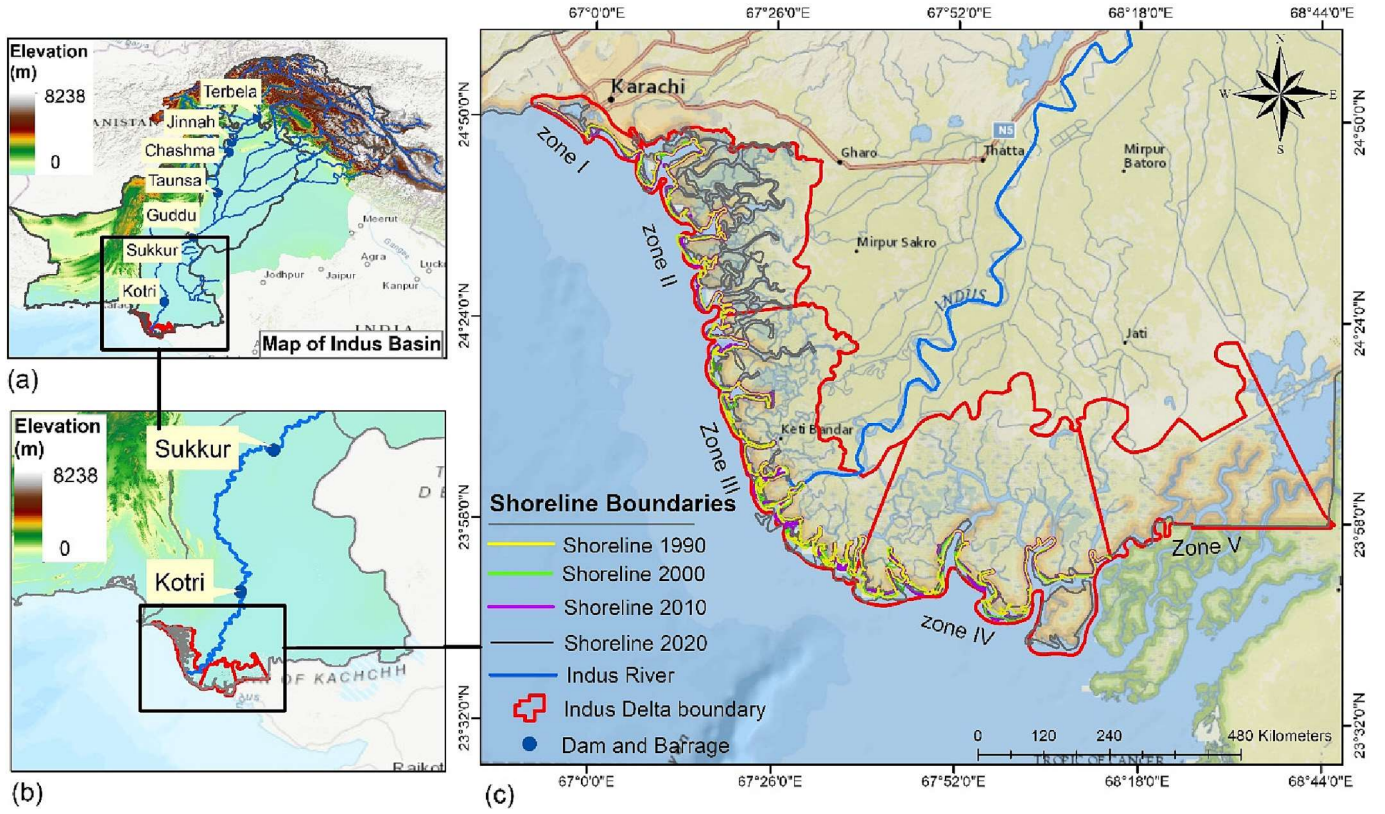

Fig. 1. Study area Map, (a). Digital elevation model of the entire Indus Basin including dams and barrages along the Indus River (b). Sindh province with Indus delta (c). Indus Delta boundary (red) with multi-temporal delineated shorelines for five different zones are shown: Zone 1 (NWK), Zone II - Western Delta (WD), Zone III - Middle West Delta (MWD), Zone IV - Middle East Delta (MED), and Zone V - Eastern Delta (ED).

world's fifth-largest Indus deltaic region and the Karachi coast (Goldsmid and Haig, 1895). The Delta also supports a population of about 1 million, distributed through 40 large and small settlements, and 20,000 tons of oil imported through coastal areas, and fishing grounds annually (Giosan et al., 2006). The lower part of the delta is characterized by an extensive system of creeks, and mangroves which spread over 1280 km^2 of area. The delta hosts the seventh largest mangrove forests in Asia, which are under pressure due to overexploitation and other factors. The coastal area for this study is divided mainly into five different zones i.e., Zone I – North-West Karachi (NWK), Zone II - Western Delta (WD), Zone III - Middle West Delta (MWD), Zone IV - Middle East Delta (MED), and Zone V - Eastern Delta (ED).

2.2. Data used

Multi-temporal Landsat data obtained by sensors (TM, ETM+ and Operational Land Imager (OLI)) and Shuttle Radar Topography Mission (SRTM) at 30 m spatial resolution was used from the USGS (http://glovis.usgs.gov) for coastline change analysis for the period 1990–2020 (Table 1). At the time of satellite data acquisition, tidal height information

Table 1
Description of satellite data, ground station data, and survey reports.

Satellite source	Acquisition time (dd/mm/yyyy)	Tidal height (m)	Shoreline length (km)	Station data	Year	Providing organization
Landsat 5 (TM)	24/10/1990	1.90	Zone I (North-West Karachi) (33.06)	Mean Sea Level data (mm)	1975–2020	NIO-National Institute of Oceanography, Pakistan
Landsat 5 (TM)	14/11/1995	2.51	Zone II (Western Delta) (180.7)	Sustain Mangroves Cover (km^2)	2000–2020	Sindh Forest Department, Pakistan
Landsat 7 (ETM+)	24/10/2000	0.23	Zone III (Middle West Delta)	Upstream Barrage flow to Delta	1937–2019	Sindh Irrigation Department, Pakistan
Landsat 7 (ETM+)	02/12/2005	1.43	Zone IV (Middle East Delta) (132.6)	**Survey Data Year Providing Organization**		
Landsat 7 (ETM+)	06/11/2010	0.13	Zone V (Eastern Delta) (151.2)	Coastal Villages Migration	2019–2021	Indus Delta Socioeconomic and Vulnerability Assessment, World Wildlife Funds for nature, Pakistan (WWF-Pakistan)
Landsat 8 (OLI)	21/11/2015	0.12	Total (651,97)	Fixed Point Photography (FPP)	2016–2020	WWF-Pakistan
Landsat 8 (OLI)	04/12/2020	0.28				

(https://www.tide-forecast.com/) was also taken into account to select the appropriate images. For identifying the erosion's impact on mangroves' sustainability, the time of neap tide satellite images was preferred because mangroves may be exposed for several hours to days and easily differentiable from other land cover features. For evaluating salinity growth in the delta, field survey data was collected using the Garmin GPS MAP 62 s

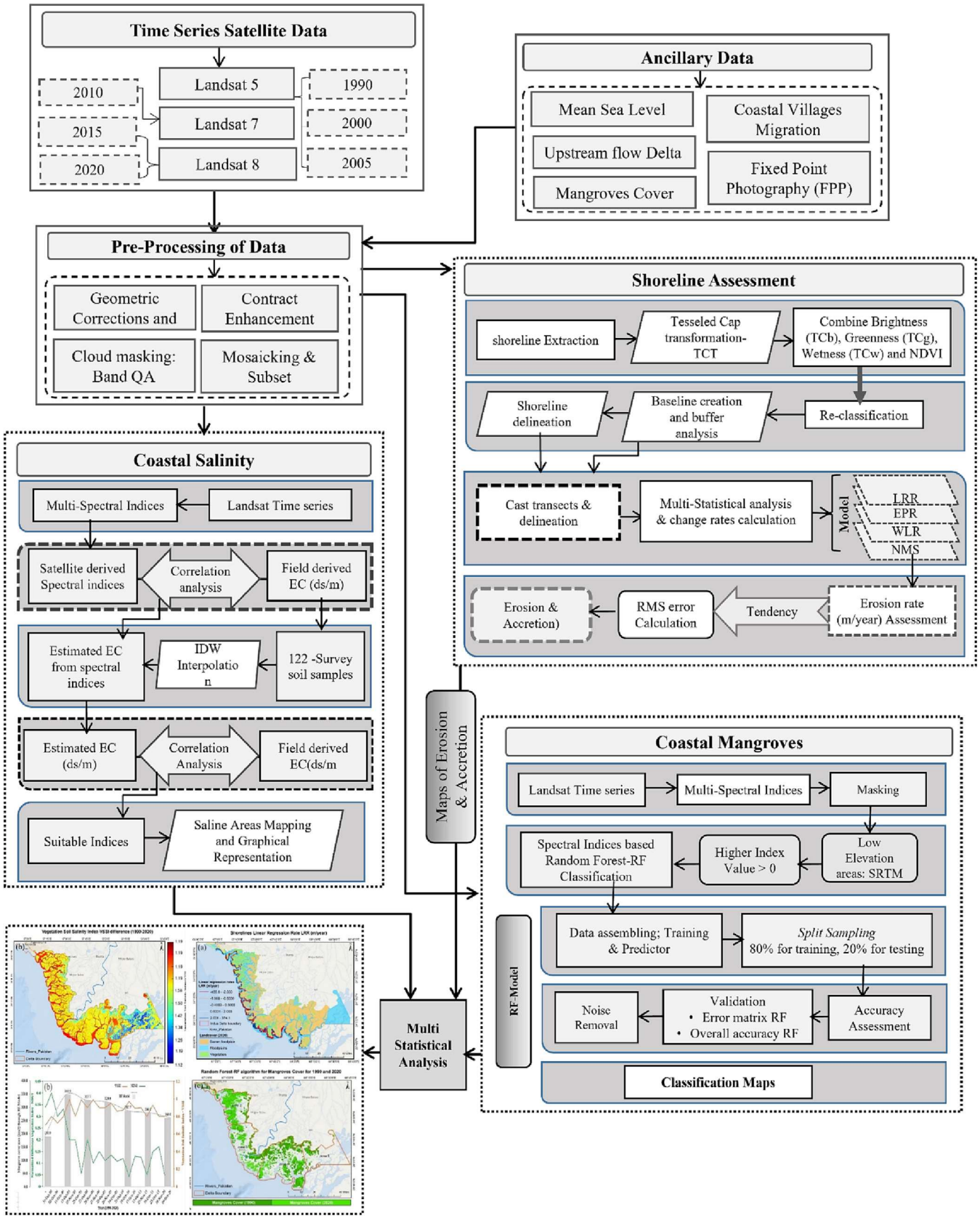

Fig. 2. Workflow for shoreline delineation and impact calculation utilizing multi-spectral indices and Random Forest classification.

system (Solangi et al., 2020). Fixed Point Photography (FPP) was used for collecting field survey data of new and degraded mangrove plantation sites for cross-verification.

2.3. Satellite image pre-processing and workflow

The overall methodology adopted for the coastline assessment and its impact on delta sustainability was divided into three parts (Fig. 2). Landsat datasets of different sensors for the study area were used to extract time series deltaic coastline assessment. All the satellite images were derived from Landsat Analysis Ready Data (ARD) collections Level-1 which have a predefined projection, co-registration, and geometrical corrections for the long-term time series analysis. The dataset was processed in the GEE, Geospatial Data Abstraction Library (GDAL) and python were used for further processing and analysis. The Landsat data quality assurance band was used to create a function to mask out clouds from the images.

2.4. Tasselled cap transformation coefficients for shorelines delineation

For the delineation of shoreline boundaries, a fully automatic TCT was used comprising of the following steps: the (a) transformation of spectral information of all bands into three principal coefficients components; (b) classification and differentiation of the land from water using principal components, i.e., brightness, greenness, and wetness coefficients; and (c) perform post vectorization between land-water raster datasets to delineate a shoreline boundary that used all water touching land pixels to create a vector shoreline boundary (DSAS, 2005).

2.5. Salinity impact on mangroves with random forest classifier and multispectral indices

Multispectral indices derived from the Landsat 30 m datasets were used to establish a relationship between coastal intrusion impacts on rising salinity in the lower deltaic estuaries. The sampled values of soil salinity were taken from the field survey conducted over the entire Indus Delta basin. A total of 122 soil samples at 40 cm depth were obtained over different land cover types which were then used for ascertaining the relationship with physicochemical parameters such as soil electrical conductivity values (Fig. 3). Indices used for this study are salinity index (SI1), salinity index (SI2), normalized difference vegetation index (NDVI), soil adjusted vegetation index (SAVI), vegetation soil salinity index (VSSI) and normalized difference salinity index (NDSI).

A correlation analysis was conducted to investigate the relationship between the collected electrical conductivity (EC) samples and spectral indices, specifically VSSI, NDSI, and SAVI (Table 2). Subsequently, a regression analysis was performed to determine which of the three spectral indices had the strongest correlation with EC.

The RF classifier was used to identify mangroves and non-mangrove cover area. The training predictors based on the multispectral indices i.e. green chlorophyll vegetation index (GCVI); normalized difference mangrove index (NDMI) (Shi et al., 2016); shortwave infrared (SWIR) and near-infrared (NIR) ratio index; NIR and RED ratio; NDVI, and modified normalized difference water index (MNDWI) for mangrove and non-mangrove forest area (Table 2).

All the samples were randomly split into 80 % for training and 20 % for the test to determine the overall accuracy. The size of the original input training data was used to select mangroves and non-mangroves data classes, using a 'bootstrap aggregating' method (Giosan et al., 2006).

3. Results and discussions

3.1. Shoreline change rate assessment

The results indicate that the mainstream part of the delta is experiencing a massive seawater intrusion. It has critical impacts on mangroves growth and water quality at the core part of the Delta, which is categorized as Zone III (MWD), and Zone IV (MED). For this study, the EPR and LRR methods were used to assess the receding shoreline positions, and the

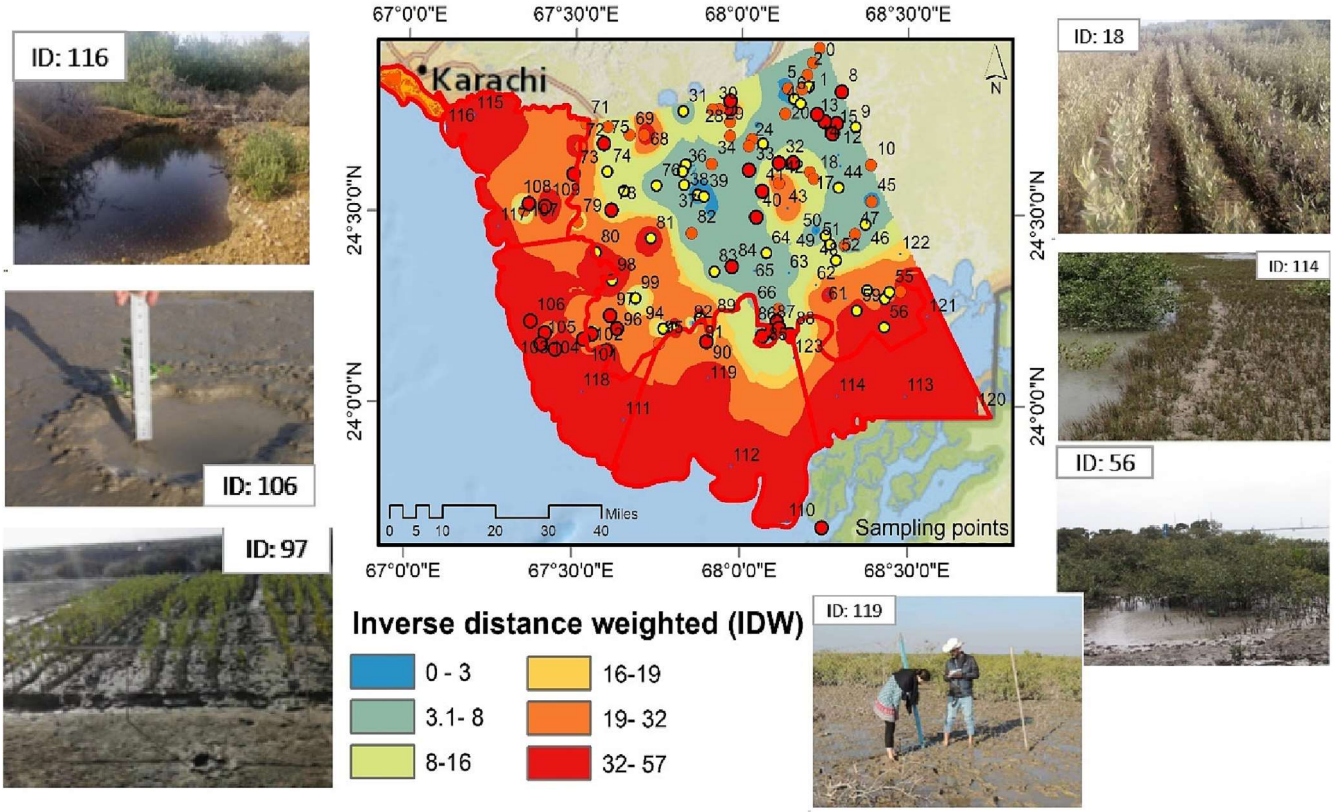

Fig. 3. Sample distribution of electrical conductivity survey (EC) conducted at different land cover.

Table 2
Spectral indices and the equations used to train the model for the identification of mangroves and non-mangrove areas.

No.	Spectral indices	Equation	Source
1	Salinity Index (S1)	$\sqrt{Green^2 + Red^2}$	(Douaoui et al., 2006)
2	Salinity Index (S2)	$\sqrt{Green * Red}$	(Douaoui et al., 2006)
3	Soil Adjusted Vegetation Index (SAVI) (L = 0.5)	$(1 + L) * \frac{NIR - Red}{L + NIR\_RED}$	(Alhammadi and Glenn, 2008)
4	Normalized Difference Vegetation Index (NDVI) Landsat 5-7 (Band 4-NIR, Band 3 - RED)	$\frac{NIR - RED}{NIR + RED}$	(Khan et al., 2005)
5	Vegetation Soil Salinity Index (VSSI)	$2 * Green - 5 * (Red + NIR)$	(Dehni and Lounis, 2012)
6	Normalized Difference Salinity Index (NDSI)	$\frac{RED - NIR}{RED + NIR}$	(Khan et al., 2005)
7	Normalized Difference Mangrove Index	$\frac{SWIR2 - Green}{SWIR2 + Green}$	(Shi et al., 2016)
8	Green Chlorophyll Vegetation Index (GCVI)	$\frac{NIR}{Green} - 1$	(Zhao et al., 2020)
9	Normalized Difference Vegetation Index (NDVI) Landsat 8 (Band 5-NIR, Band 4 -RED)	$\frac{NIR - RED}{NIR + RED}$	(Khan et al., 2005)
10	Normalized Difference Water Index (NDWI)	$\frac{Green - NIR}{Green + NIR}$	(Gao, 1996; Khan et al., 2005)

assessment was made at five different Zones. A total of 16,049 transects were generated at 1 km intervals starting from the west, 826 for Zone I (NWK), 4516 in Zone II (WD), 4505 for Zone III (MWD), 4141 for Zone IV (MED), while 2061 transects were formed in Zone V (ED).

3.1.1. Zone I (NWK): accretion and erosion analysis

The quantified results of the transect map were delineated along the coastal stretch of Zone I at the western site via change cover assessment joining the LRR rates and creek name attributes shown in Fig. 4. Besides this, 23.24 km of land showed accretion near the Kajhar creek area. The average observed progressive rate was 7.28 ± 1.15 m/year recorded at the Sandspit area, and the process of accretion was dominant along the western coast. Overall estimated shoreline change rate was with mean LRR of 17.21 and 11.99 m/year (Fig. 4), with an increment in positive values. The statistical results showed that LRR is positive for Zone I particularly towards the Kajhar creek area with an observed +17.21 m/year change rate. Whereas a small amount of erosion with −0.13 m/year was observed around the Wari creek area.

3.1.2. Zone II (WD): accretion and erosion analysis (1990–2020)

The results obtained from the Zone II (Western Delta) coastline assessment indicate it is a highly risked area towards erosion with an average LRR −10.09 ± 1.61 m/year, mainly contributed by receding properties of land towards the sea (Fig. 5). Results also indicate has high erosion at the Phitii creek area with an average rate of −33.95 m/year, −37.36 m/year for Rahu creek, −51.20 m/year for Waddi creek experienced tremendous erosion and -3.26 m/year at the Pitiani creek, respectively for the last three decades (1990–2020). Moreover, out of the 180.7 km area, the highest observed erosion rate was at Phitii, Rahu, and Waddi creek by about 148.8 km, where the land was badly eroded along the western coast.

Rapid consideration and action are needed in this zone, according to the survey report of environmental threats in Indus delta villages, in Pakistan (Mallah, 2013).

3.1.3. Zone III (MWD): accretion and erosion analysis

Zone III has also experienced erosion during the time of the last thirty years (1990–2020) and out of 155.6 km area, 120 km land was eroded at −13.52 ± 1.75 m/year rate and the 35.6 km area showed advancement in shoreline position (Fig. 6). The highest erosion was observed at the eastern side of Daboo creek with an average rate of −26.9 m/year at a 10 km area. Chann and Bhuri creek is also undergoing recession with an average −14.78 m/year rate. Based on the shoreline change rate analysis (Fig. 6), Hajamaro/Orchito creek near Keti Bandar area (intersection point of Indus River and Arabian sea) exhibits a high erosion towards land with an average −14.39 m/year cumulative rate from west to east. This receding property of land had an adverse influence on the coastal mangrove canopy in the delta due to land intrusion at a −21.64 m/year rate.

To effectively manage the coastal erosion hazard in the following creeks areas of Hajamaro/Orchito and near Keti Bandar, it is crucial to regularly monitor and assess the coastline changes, particularly in the vulnerable areas. The transect-based coastline change rate analysis method used in this study provides valuable information on the erosion rates of different creeks and banks, which can aid in identifying high-risk areas and developing appropriate risk management strategies.

For instance, the areas at the east of Chann Creek mouth to Wari Creek in the subzone, which have experienced an average erosion rate of −14.75 m/year, could be prioritized for risk mitigation measures such as beach nourishment, dune restoration, or artificial reef construction. Similarly, the transects showing mixed signs of accretion and erosion, such as the East Hajamaro creek banks, could be monitored closely to detect any further changes in the erosion rates and take prompt action if necessary.

Overall, a proactive approach towards risk management, including regular monitoring, timely intervention, and stakeholder participation, can help mitigate the negative impacts of coastal erosion and promote sustainable development in the Indus River Delta region.

3.1.4. Zone IV (MED): accretion and erosion analysis

The central part of the lower deltaic is between the east-west coastlines of the Indus River. From the total 132.6 km area, 50.2 km of Land is reaching up to −9.63 ± 2.3 m/year erosion rate as shown in supporting Fig. S3 (attached as a separate file). The 82.4 km of land showed advancement with an average 45.60 m/year rate at the eastern side of Mal creek, where erosion rates were distinct, compared to the western sides of lower mudflats. Overall, the average erosion rate was found to be highly receded towards Mal creek with an average −34.08 m/year rate (Fig. S3), which also indicates the deltaic soil primarily consists of marshy mudflats and easily be eroded by sea waves at Middle East side of the delta. The area near Chann creek is also experiencing erosion with −15.60 m/year. Wari creek showed a high rate of erosion, reaching up to −34.9 m/year from the Indus River to the eastern location of Wari Creek and mangrove cover on small patches along coastline marginal grazing lands was lost due to intensifying vulnerabilities.

3.1.5. Zone V (ED): accretion and erosion analysis (1990–2020) and assessment

The estuaries at the extreme eastern side of the delta, including the Wari and eastern Kajhar creek sub zonal areas near the coastline, have been less eroded and sustained during the last three decades with an average rate of 8.13 ± 1.65 m/year as shown in supporting Fig. S4 (attached as a separate file). Furthermore, the coastline at the Indus River mouth (Keti-Bandar) was found to be less encroached by the saltwater salinity and the sustainable mangrove forest found here. This zone is hence resistant to the land loss processes, particularly in the eastern deltaic creeks (i.e., East Wari creek, Kajhar creek, East Kajhar creek) with less inundation. The accreting properties of coastal land consequently increased the total cross-sectional area of zone V (ED) for mangrove forests, particularly near those areas where tidal action can be strong. Consequently, the eastern deltaic zone

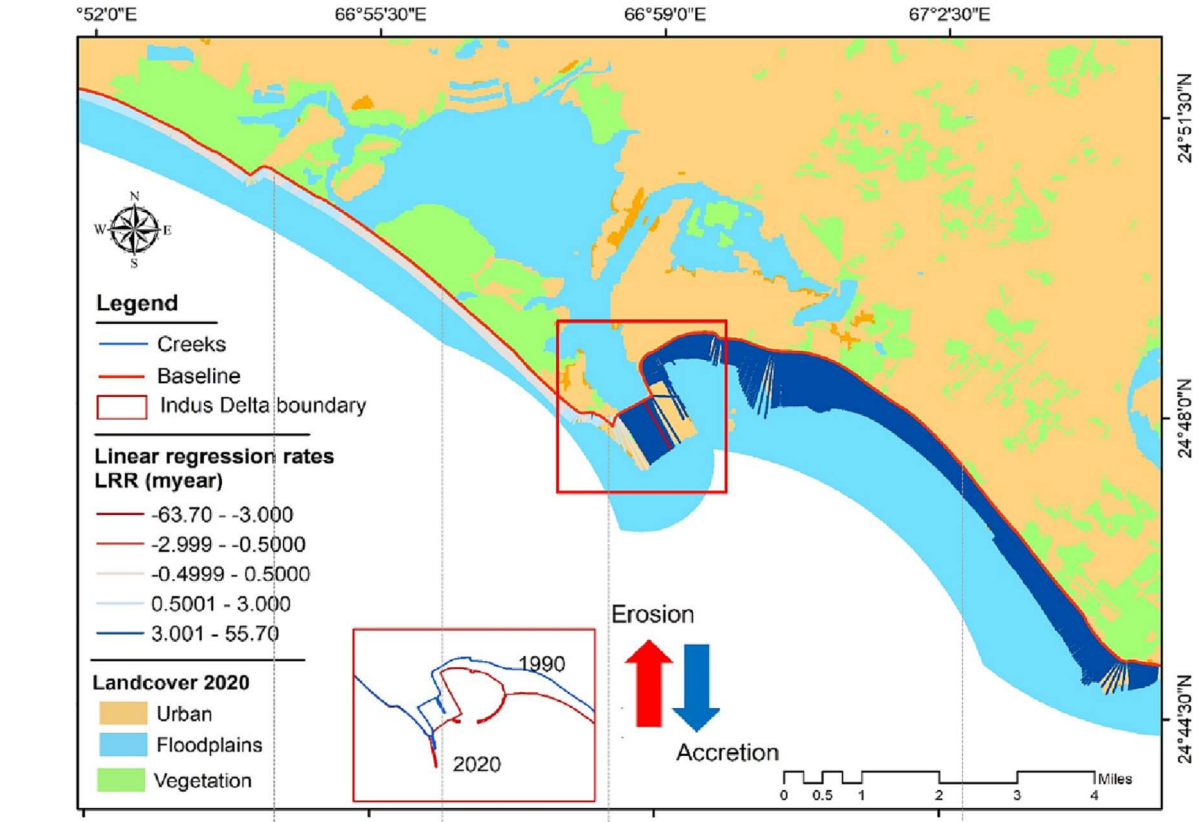

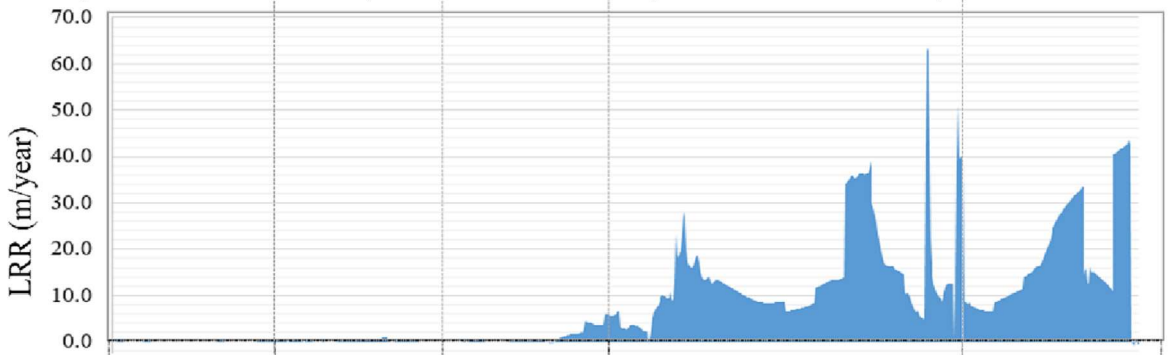

Creek Name	Wari Creek	East Wari	Kajhar Creek	East Kajhar
Intrusion type	Accretion	Accretion	Moderate accretion	Erosion
Location	East delta	East delta	East delta	East delta
Mean LLR (m/year)	-0.13	+0.05	+17.21	+11.99
Action	Not Essential	Not Essential	Essential	Not Essential

Fig. 4. Shoreline analysis and risk assessment at the western side (Sandspit, Karachi) for the NWK by LRR between 1990 and 2020 with creek names and intrusion type.

reduces the vulnerability risk to climate-induced coastal hazards and has increased the resilience of coastal communities, particularly towards east Kajhar creek.

The information about the accretion at the eastern and western deltaic regions was also verified through already conducted studies (Crist, 1985) during the period 1984 to 2016. However, the majority

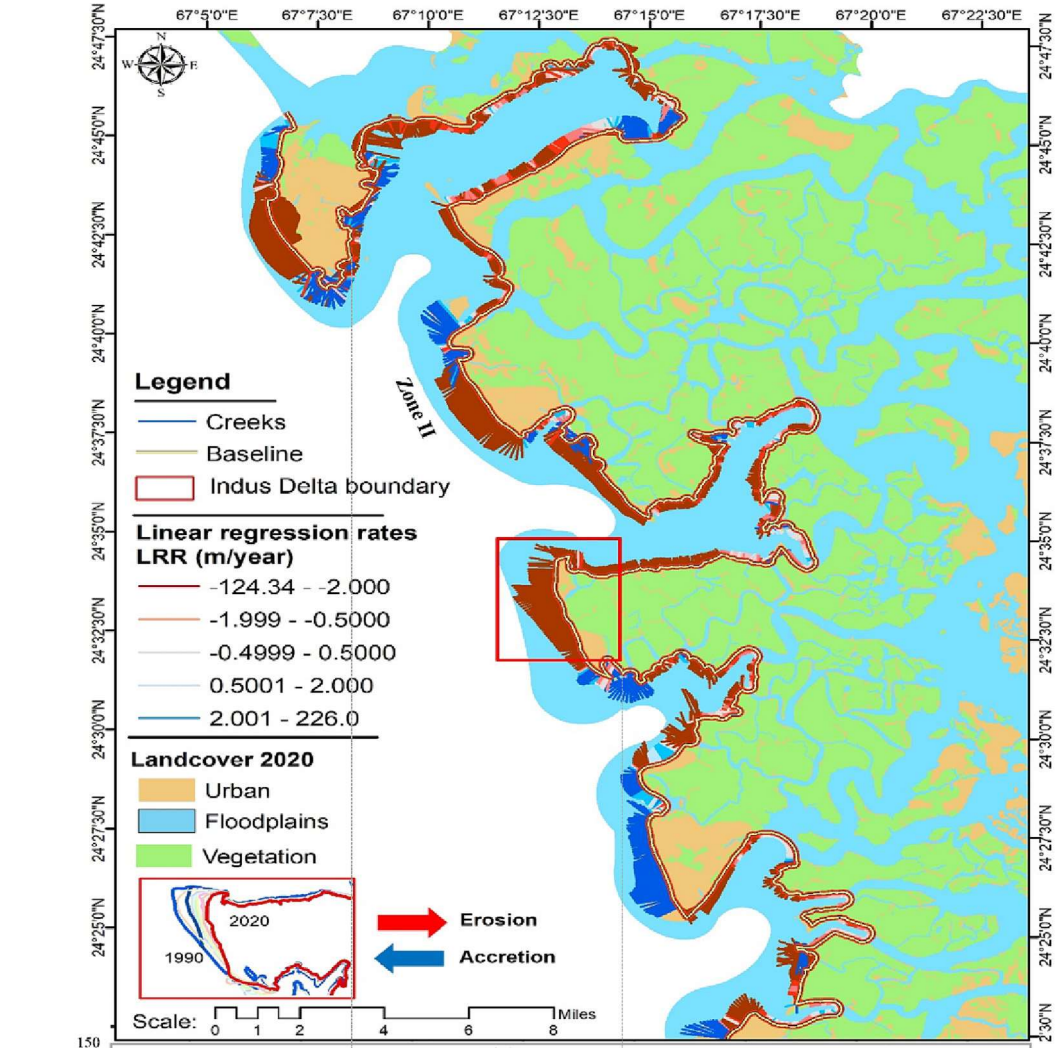

Creek Name	Phitii & Jhari Creek	Jhari Creek	Rahu Creek	Waddi creek	Khal creek	Pitiani Creek	East-Pitiani
Intrusion type	High erosion & accretion	Moderate accretion	Very High erosion	Very High erosion	High accretion	Erosion	Accretion
Location	West delta	West delta	West delta	West delta	West delta	West delta	West delta
Mean LLR m/year	-33.95 & +4.01	+28.719	-37.36	-51.20	+23.22	-3.26	+3.18
Action	Essential	Not Essential	Rapid Essential	Rapid Essential	Not Essential	Not Essential	Not Essential

Fig. 5. Shoreline analysis and risk assessment at the western side for the WD by LRR between 1990 and 2020 with creek names and intrusion type.

of the Land in Zone II was receding towards land with an average −10.09 ± 1.61 m/year rate due to saltwater intrusion at Jhari/Rahu and Waddi/Pitiani creek area which have also been verified by (Kanwal et al., 2019), with an average calculated rate of −14.174 ± 0.55 m/year. The erosion trend in Zone II is also in line with studies by (Din Hashmi and Ahmad, 2018; Waqas et al., 2019) on coastal assessment and showed Jhari/Rahu Waddi/Pitiani creek is eroding at very high rates.

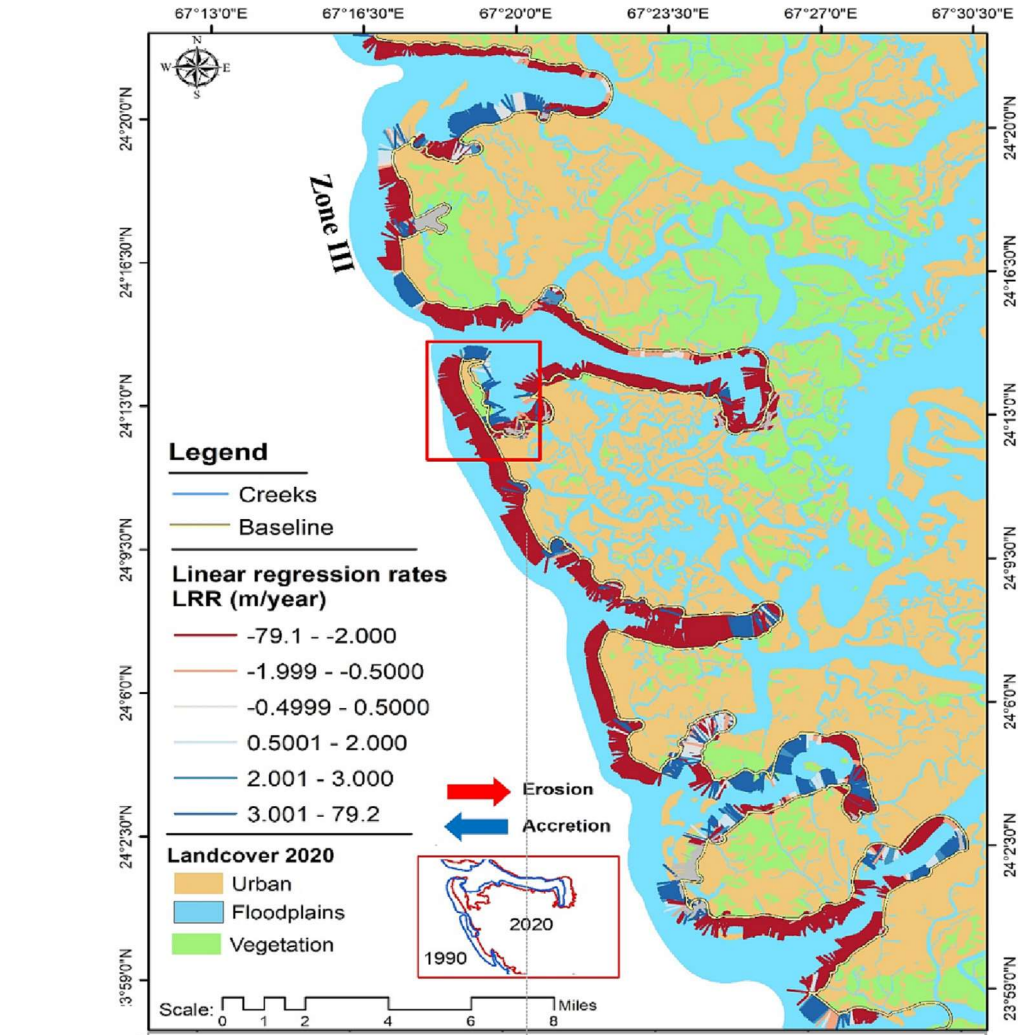

Creek Name	Daboo Creek	East-Daboo	Chann & Bhuri Creek	Hajamaro & Ochito Creek	East Hajamaro	Khober Creek
Intrusion type	Erosion & Accretion	High erosion	Moderate erosion	Moderate erosion	Accretion	High erosion
Location	Mouth of Delta	Mouth of Delta	Mouth of Delta	Mouth of Delta (Keti bandar)	Mouth of Delta	Mouth of Delta (Indus River)
Mean LLR (m/year)	-8.19 & +8.5	-26.9	-14.78	-14.39	4.74	-21.64
Action	Essential	Rapid Essential	Rapid Essential	Rapid Essential	Not Essential	Rapid Essential

Fig. 6. Shoreline analysis and risk assessment at the mouth of the Indus delta with creek and intrusion type attribute values for the MWD by LRR between 1990 and 2020.

The Hajamaro/Orchito creek area in front of active Indus River mouths between Chann creek and east Hajamaro creek (Keti Bandar region) is also found to be highly encroached by saltwater intrusion from Arabian sea respectively. The finding of this sub-Zone Keti Bandar area is then compared with already conducted studies (Giosan et al., 2006; Kanwal et al., 2019; Solangi et al., 2020) showed high consistency in experimental

results. Moreover, the continuous decrease in sediment flow and the land receding processes particularly at the Middle Western side along the creek banks destroyed a massive amount of mangrove cover, particularly where tidal action near the coastline area of Keti Bandar is strong. The process of meandering within creek areas is also one of the factors responsible for the degradation of mangroves was also discussed (Mukhtar and Hannan, 2012). The results of erosion in Zone IV (MED), at west Mal creek, were also compared with (WWF-Pakistan, 2005), which is in line with findings of a −23.89 m/year erosion rate conducted between 1952 and 2006. Khober creek area showed an annual change rate of −34.9 m/year from 1990 to 2020, with an initial rate of −10 m/year from 1895 to 1952, according to the morphodynamics studies of the Indus delta (Giosan et al., 2006). Zone IV, Chann creek showed erosion −15.61 m/year which is also compared to the Indus erosion studies where the coastline is receding landward and in line with the findings of previous condcuted studies (Waqas et al., 2019).

3.1.6. Coastal assessment and validation

For the coastal area assessment, shoreline extraction and its validation were one of the crucial and probably more difficult parts, especially when no up-to-date reference datasets available in such an inaccessible and undeveloped large lower deltaic region. To evaluate the shoreline accuracy, the 2015 boundary provided by WWF; retrieved from high-resolution imagery coincide with the acquisition date of the Landsat data. Root Mean Square Error (RMSE) was estimated between the referenced and calculated shoreline positions for validation and estimating error using an RMSE.

$$\mathrm{RMSE} = \sqrt{\frac{1}{n}\Sigma_{n=1}^{n}(X_{cal} - X_{ref})^2 + (Y_{cal} - Y_{ref})^2}, \quad (1)$$

where 'X_{cal}' and 'Y_{cal}' indicates the coordinates of the calculated shoreline at each transect in the x and y position which is cast at a 1 km distance. 'X_{ref}' and 'Y_{ref}' are shoreline coordinates obtained through reference shoreline e.g. (high-resolution IKONOS ~0.82 m) at each transect, whereas 'n' is for transect number. After that, the correction was applied according to the shift in the x and y position as follow:

$$X_{\text{Correction rate}} = \frac{X_{Ref} - X_{cal}}{\text{Time Interval}}; Y_{\text{Correction rate}} = \frac{Y_{Ref} - Y_{cal}}{\text{Time Interval}} \quad (2)$$

From Eqs. (1) and (2), time was defined as the interval between the calculated and referenced shoreline, and then correction in X and Y was applied for the accurate shoreline delineation. The total difference in the reference shoreline was compared with the extracted one obtained from the Landsat imagery and the value of displacements estimated at each transect using shoreline data. The positional error varied from −37.4 m to 26.3 m. It has been found that model prediction error is homogeneous in all the shorelines. The overall RMSE for the future predicted shoreline in 2015 measured 17.54 m. The correction error was applied to calculated shoreline rates and the ones calculated from Landsat data (Fig. 7).

3.2. Time series impact on mangrove extent

Changes in mangrove cover at the five different zones of the delta were related to changes in shoreline position (Fig. 8). Shoreline changes were calculated through LRR (Fig. 8a) salinity difference through VSSI index (Fig. 8b) and mangroves change detection was studied by the machine learning RF algorithm (Fig. 8c). Due to the increase in the shoreline at NWK, the total mangrove has increased from 11.0 km^2 in 1990 to 14.5 km^2 in 2020 with an annual 3.5 km^2 area difference. However, total mangrove cover was reduced from 11.0 km^2, in 1990 to 9.81 km^2 in 1995, with an annual change of 1.21 km^2 and later increased from 11.8 km^2 in 2010 to 14.5 km^2 in 2020. In the case of Zone II (WD), mangrove cover was estimated at 190.0 km^2 area in 1990, and increased to 220.6 km^2 in 2005, with an annual area change difference of 30.6 km^2 (Table 3). Out of a total of 387 km^2 of mangrove area in 2010, 107 km^2 of mangrove cover was degraded by seawater intrusion and become a part of tidal floodplains.

Zone III (MWD), the mouth of the delta experienced a high rate of saltwater intrusion due to a decrease in sediment deposition in the mouth of the deltaic. This middle west side has experienced mangrove loss at 96.1km^2 area from 1990 to 2020 due to a diminution in sediment flow from 56 to 0.05 (BCM) near Hajmaro creek (Fig. 12). Furthermore, 0.4 km^2 changed between 2010 and 2015, and finally, 0.5 km^2 of mangrove area degraded from 2015 to 2020 (Table 3).

Mangroves cover in MWD decreased from 90.8 km^2 in 1990 to 85 km^2 area in 2020. The change detection map of Zone IV in Fig. 8e indicates a loss of a distinct mangrove belt, along the middle east side of the shoreline which acts as a barrier against cyclones, coastal erosion, and a fence against the intruding salinity problems to coastal communities. Zone V (ED) was found the most sustainable zone of the lower Indus delta with progressive shoreline characteristics and the land is accreting towards the sea. Moreover, the maximum mangrove growth rate was observed (an increase of 775 km^2) from 1990 to 2020 with a 775 km^2 area difference (Table 3). The total cover was 221.4 km^2 in 1995 which further increased to 340 km^2 in 2000. Moreover, the mangrove area has further increased to 370.3 km^2 in 2005, with a total 305 km^2 area difference from 1990 to 2005.

The environmental factors considered are the frequency and severity of erosion, which can significantly affect mangrove distribution and growth. Fig. 8 provides an integrated assessment of saltwater intrusion on mangroves, highlighting the most vulnerable areas (Zone III and Zone IV in Fig. 8e) and providing support for informed management strategies. In the end, accuracy assessment was performed through kappa coefficients and the results of shoreline change rate are then compared with annual mangrove cover in the lower delta estuaries from the already conducted studies (Fig. 9).

The findings of this research also showed the spatiotemporal changes in mangrove cover along the shoreline. Rapid coastal erosion has destroyed the woody coastal mangrove belt, particularly near the strong tidal area, and additional salinity sediment deposits were also the reasons for mangrove degradation (Giri et al., 2011). The mangrove change rate assessment is also endorsed by the information provided by several other studies (Gilani et al., 2021; Abbas et al., 2012, 2013; Giri et al., 2014; WWF-Pakistan, 2005).

The summary obtained from Figs. 8 and 9 shows the changes in shoreline and mangrove cover across five different zones of the lower Indus Delta using a multi-temporal Landsat imagery and Random Forest machine learning approach. Zone II coastline assessment was categorized as a highly risked area towards erosion and leading to a loss of mangrove cover. A study conducted in the Indus delta (Dasgupta et al., 2018) also reported the complete disappearance of a mangrove patch along the coastal Indus delta due to seawater intrusion, highlighting the vulnerability of mangrove ecosystems in the Indus Delta to such stressors. However, Zone IV was found to be the most sustainable with progressive shoreline characteristics and an increase in mangrove growth rate with several recent studies also highlighted the positive trend of mangroves in the Indus Delta. (Giri et al., 2011; Qureshi et al., 2019) both reported significant increases in mangrove cover in the entire delta, with a 29.5 % increase observed from 1990 to 2016 (Ahmed et al., 2021) also found evidence of mangrove regeneration and reforestation efforts, with increases in mangrove cover observed in various areas of the delta. Additionally, the study conducted over the past 15 years (2005–2020) showed a significant increase in mangrove cover, from 804.65 km^2 in 2005 to 1395.66 km^2 in 2020 (Gilani et al., 2021). Although the overall extent of mangroves in the Indus Delta has increased over the past fifteen years, there has also been an increase in mangrove loss, particularly in Zone II and Zone III. These areas are experiencing significant seawater intrusion, which is affecting the growth of mangroves. Therefore, the authors of these studies highlight the critical importance of protecting and restoring mangrove ecosystems in the face of ongoing threats from human activities and climate change.

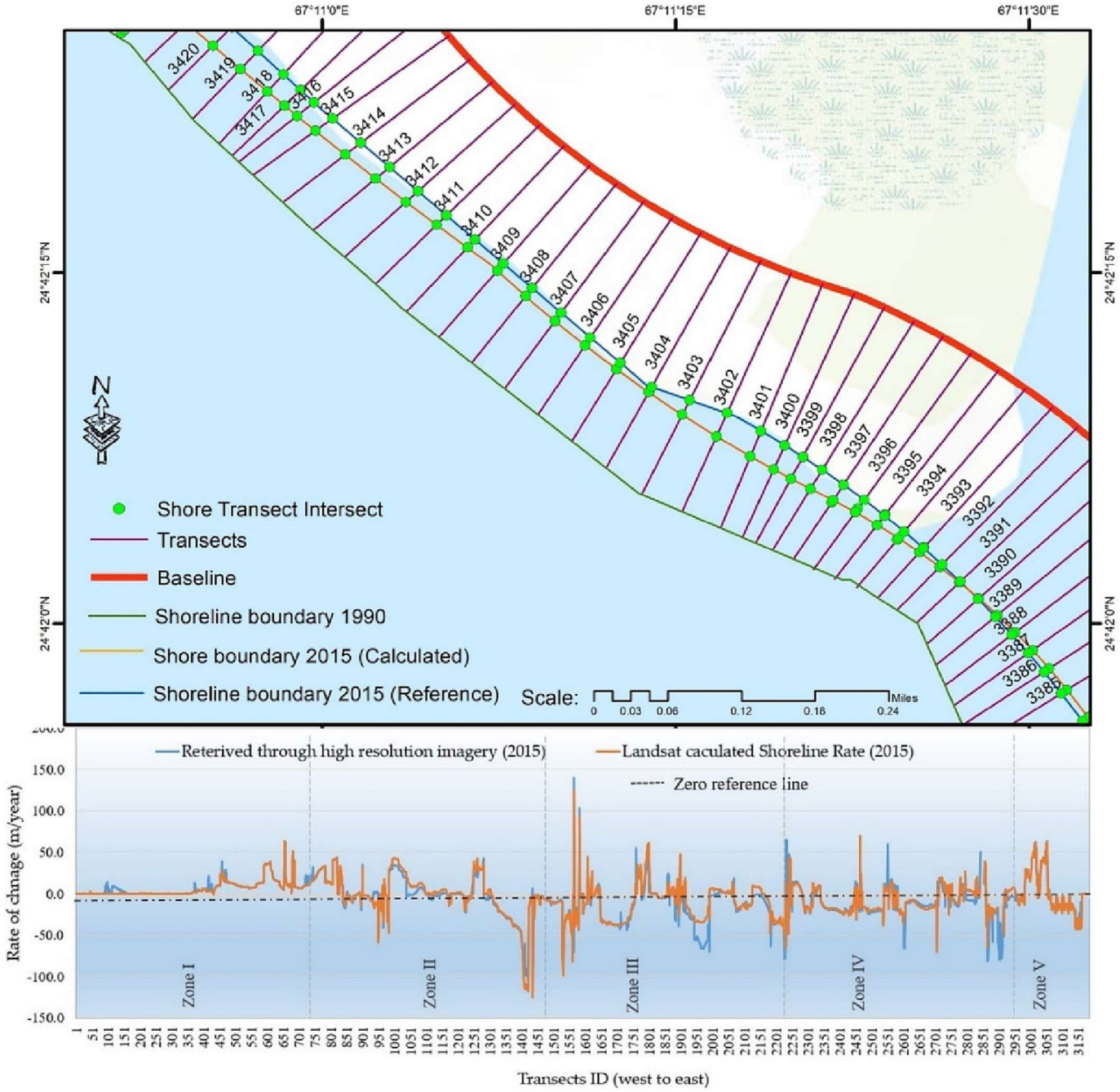

Fig. 7. Calculated and Reference shoreline rates (m/year); transect numbering from west to east, baseline (red), calculated shoreline (orange), reference shoreline (blue).

3.3. Estimation of the soil salinity and accuracy assessment using the VSSI

The results obtained from the spectral indices derived from remote sensing data and the corresponding regression models showed the VSSI and NDSI showed the highest correlation to the salinity values obtained from the field measurement. The highest coefficient value $R^2 = 0.83$ was obtained through VSSI (Fig. S5). The highest correlation between VSSI-derived EC (dS/m) and field/observed EC (dS/m) values were obtained through the regression model. The correlation (R^2) between EC and VSSI and between EC and NDSI was 0.83 and 0.57, respectively and the least correlation exists in SI1, SI2, and NDVI indices as shown in supporting Fig. S5 (attached as a separate file). Hence, the results indicate the VSSI model was the most suitable one for the salinity area mapping when compared with the other indices (Fig. 10).

Zone II and Zone III showed a significant variation in salinity growth (Solangi et al., 2023), which was mainly influenced by rapid coastal intrusion and a decrease in upstream river discharge, as also discussed in a study conducted on the Indus Delta (Nasir and Akbar, 2012). In 2020, the maximum variation in salinity was observed from 1.68 to 1.83 along the coastline and values were accelerated towards Zone II, Zone III, and Zone IV. During the year 1990, VSSI varied between a range of 0.42 to 1.06 which then accelerated from 0.98 to 1.29 in the 2010 year (Fig. 11).

In 2010, the vertical distribution of sediment flow from the Kotri barrage was reduced from 50 (BCM) to 0.05 (BCM) (Fig. 12) and the highest values of salinity were recorded near Zone III. Rapid construction of upstream barrages and dams (Fig. 12) is one of the major factors towards land erosion with rising salinity problems from the Arabian sea.

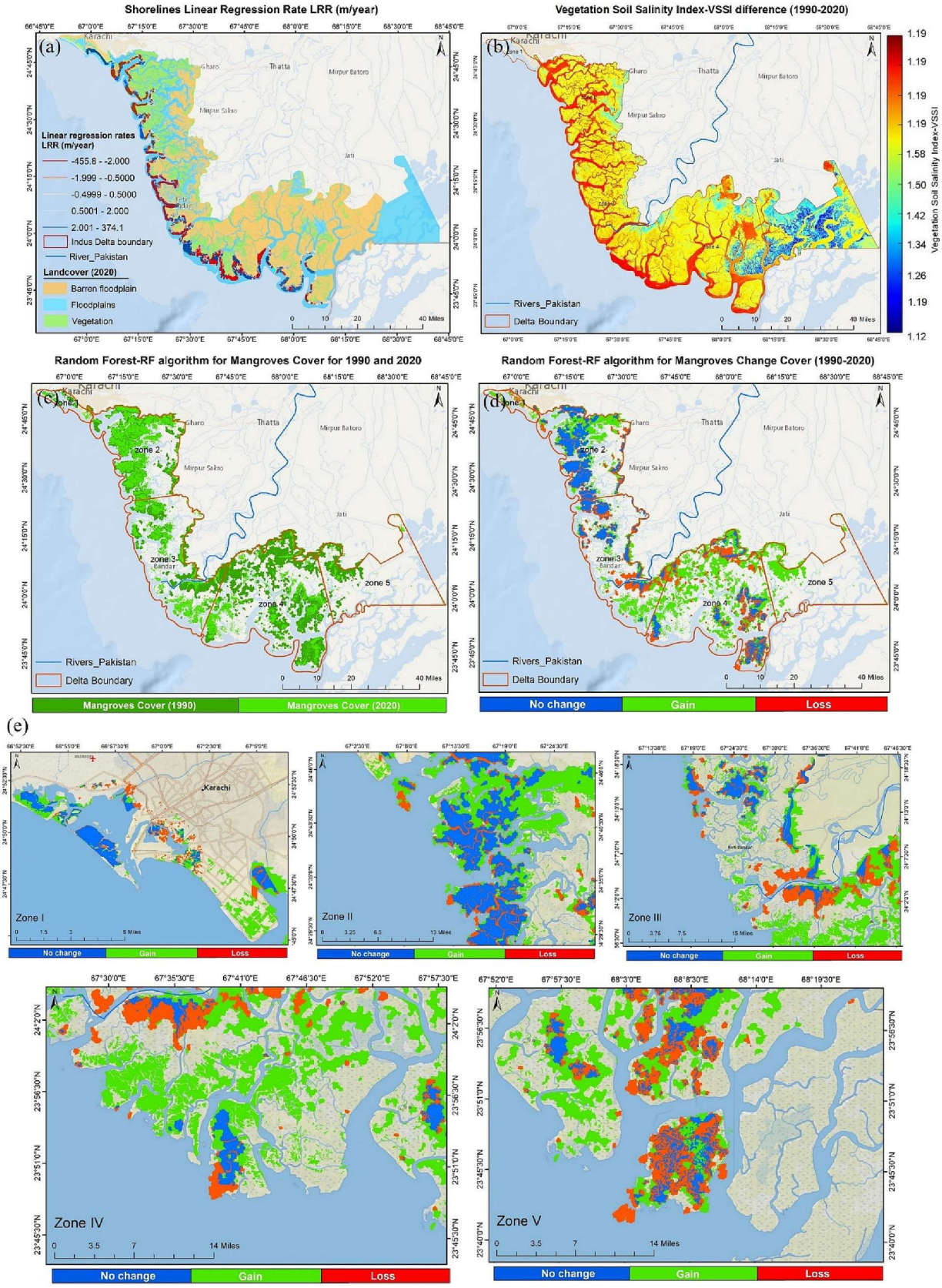

Fig. 8. Integrated assessment of saltwater intrusion and mangrove change cover over a period (1990 to 2020); (a) shoreline change rate estimation using Linear regression rate (LRR), highlighting areas of erosion and accretion; (b) the impact of saltwater intrusion on salinity, measured by Vegetation Soil Salinity Index (VSSI); (c) mangrove change cover, with green indicating mangrove gain, blue indicating no change, and red with mangrove loss; (d) a breakdown of mangrove change cover, showing the percentage of the area experienced mangrove loss, gain, and no change; (e) mangrove change assessment at different spatial scales, with specific zones of interest.

Table 3
Mangrove forest classification results (km^2) from RF-Model 1990, 1995, 2000, 2005, 2010, 2015 and 2020.

Time	1990	1995	2000	2005	2010	2015	2020
ZONE I: NWK - (Wari Creek, Kajhar Creek)							
Mangrove cover (km^2)	11.0	9.8	9.9	10.0	11.8	11.5	14.5
Average distance from baseline (m)	150.3	189.1	190.23	199.9	205.27	215	288.4
Average shoreline change rate (m/year)	7.28 ± 1.15 m/year						
Overall accuracy (%)	96	97	96 97		95	98	98
Kappa coefficient	0.95	0.94	0.95	0.95	0.92	0.95	0.97
ZONE II: WD - (Phitii Creek, Jhari Creek, Rahu Creek, Waddi Creek, Khal Creek, Pitiani Creek)							
Mangrove cover (km^2)	190	188.9	222.7	220.6	387.7	280	260
Average distance from baseline (m)	1300	987	875	754	501	407	135
Average shoreline change rate (m/year)	−10.09 ± 1.61 m/year						
Overall accuracy (%)	98	95	97	95	94	98	97
Kappa coefficient	0.95	0.96	0.94	0.93	0.95	0.98	0.96
ZONE III: MWD - (Daboo Creek, Chann Creek, Hajamaro Creek, Khober Creek)							
Mangrove cover (km^2)	180	110	119.7	98	84	84.4	83.9
Average distance from baseline (m)	443	419	398	317.1	255.2	201.2	175
Average shoreline change rate (m/year)	−13.52 ± 1.75 m/year						
Overall accuracy (%)	98	97	98	97	96	98	98
Kappa coefficient	0.96	0.98	0.97	0.96	0.93	0.97	0.96
ZONE IV: MED - (Sunhri Creek, Kahar Creek, Mal Creek, Wari Creek)							
Mangrove cover (km^2)	90.0	98.7	68.6	78	89	85	76
Average distance from baseline (m)	1231	908	789	501	423	298.2	169
Average shoreline change rate (m/year)			−9.63 ± 2.35 m/year				
Overall accuracy (%)	98	95	96	98	95	97	98
Kappa coefficient	0.97	0.93	0.97	0.96	0.94	0.98	0.97
ZONE V: ED - (Wari Creek, Kajhar Creek)							
Mangrove cover (km^2)	75	221.4	340	370.3	390	499	850
Average distance from baseline (m)	1551	1498.2	1470.1	1424.2	1389.9	1372.3	1368
Average shoreline change rate (m/year)	8.13 ± 1.65 m/year						
Overall accuracy (%)	97	96	98	97	98	96	97
Kappa coefficient	0.98	0.95	0.96	0.98	0.95	0.95	0.96

The increase in salinity spatially has been mapped out using the VSSI index during the year 2020 where the river discharge was almost negligible; therefore, a salinity penetrated a longer distance upstream in the lower delta; and shaped a strong salinity stratification at the lower estuary. After the construction of a major dam in Pakistan in 1968 (Tarbela dam) and 1962 (Guddu barrage) along the Indus River significantly and mainly reduced river discharge (Fig. 12), thus reached its highest value during the year 2010 (Nasir and Akbar, 2012).

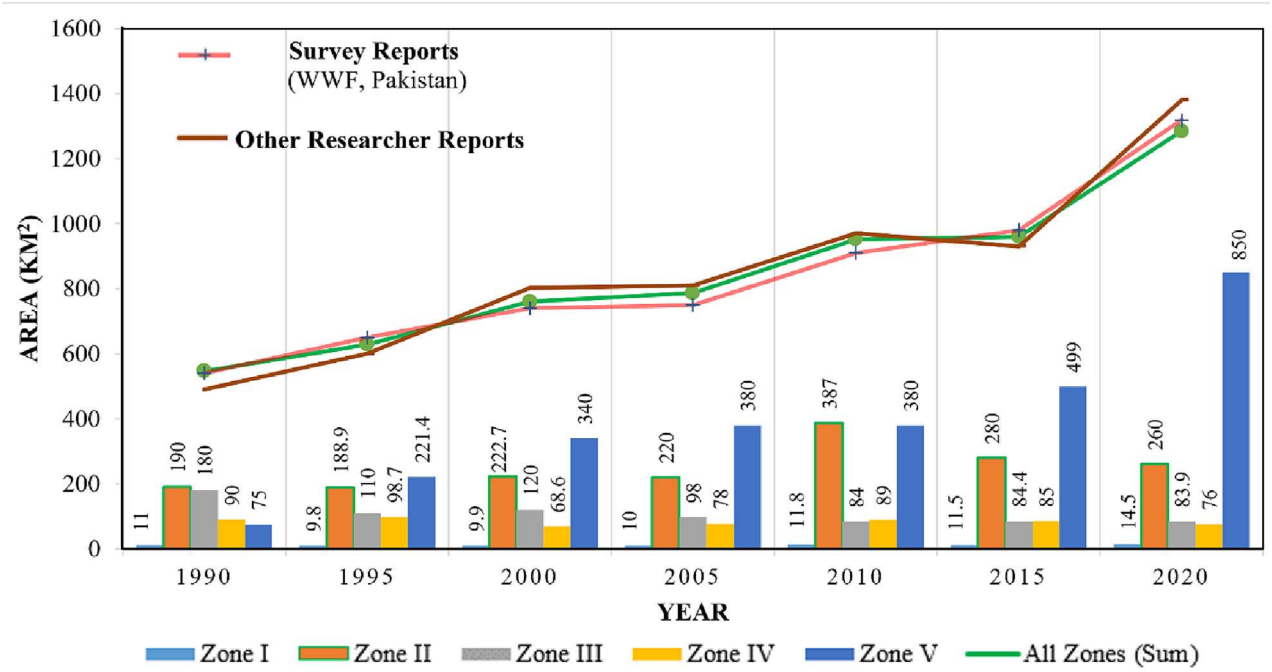

Fig. 9. Mangrove cover in each individual zone, including Zone I (NWK), Zone II (WD), Zone III (MWD), Zone IV (MED), and Zone V (ED), with the sum of all zones indicated by the green color line, red line shows the annual mangrove cover retrieved from the WWF survey report, brown color line indicates a comparison with global-scale conducted studies from 1990 to 1995 (Gilani et al., 2021); 2000 (Giri et al., 2014); 2005 to 2010 (Solangi et al., 2020) and between 2015 and 2020 (Bunting et al., 2018).

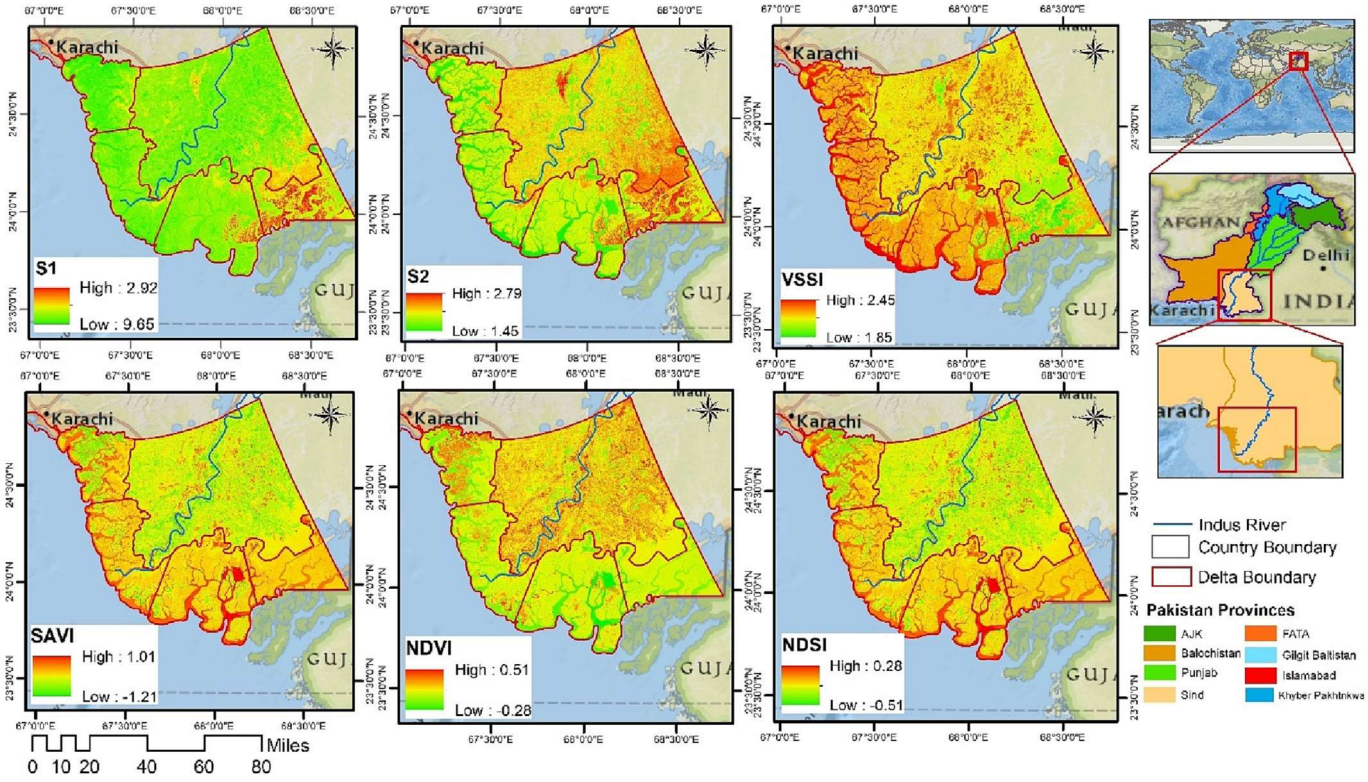

Fig. 10. Multispectral salinity maps derived from Landsat using SI1, S12, VSSI, SAVI, NDVI and NDSI channels; (Basemap Credits: Esri, Garmin, OpenStreetMap contributors, National Geographic, USGS).

3.4. Statistical comparison

The relationship between NDVI and VSSI indicates that higher values of salinity lead towards low NDVI. However, the RF-Model for mangrove calculation showed a positive correlation with NDVI values with an increase in mangrove cover which showed high values of NDVI, and low salinity observed values for NWK and ED.

On the other hand, for Zone II (WD), Zone III (MWD), and Zone IV (MED), the highest values of salinity were found with the least corresponding mangrove cover near the coastline. The central part delta is deficient the most in terms of mangrove cover and Greenland due to intruding salinization from the Arabian sea which negatively affects the plants' growth. The statistical relationship between RF classifier with NDVI values and VSSI for Zone I is shown in Fig. 13 during the time 1990 to 1995 and it experienced a loss in mangrove canopy with low NDVI reflectance values and rising VSSI salinity values. During the period 1995 to 2015, Karachi's west side recorded a consistent increase in vegetation values from 0.2 to 0.3, and the salinity reduced from 1.4 to 1.1. At Zone II (WD), due to land degradation, salinity upstretched from 0.75 to 1.0 with a decrease in NDVI values from 0.3 to 0.05. On the other hand, high values of mangrove cover with NDVI values were recorded in the middle west region, during the time 1990 to 2005 with a high mangrove canopy cover ($0.7 < NDVI < 0.9$). The resultant statistical relationship is thus indicating the severe scale impact of coastal intrusion on salinity with mangrove growth and demarcates its relationship which gradually decreases the availability of the appropriate environment to increase mangrove cover and soil productivity in the natural ecosystem.

3.5. Monitoring through Fixed Point Photography (FPP)

FPP helped to identify exact locations and mangrove cover changes. Fig. 14 pronounced the FPP was taken at the part of the lower Indus delta mainly in the middle east and west part of the Indus Delta from May

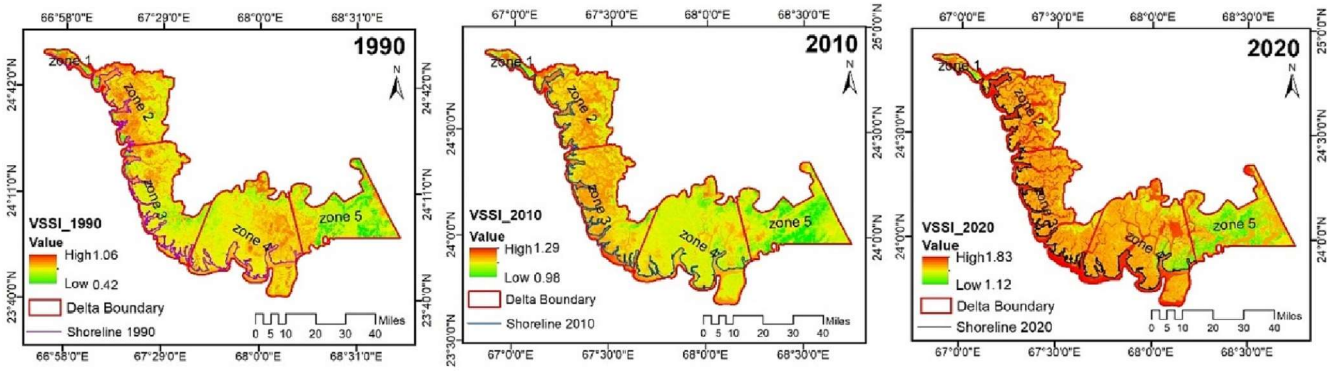

Fig. 11. Soil salinity map at the lower Indus deltaic estuary, using the VSSI index for the period 1990, 2010 and 2020.

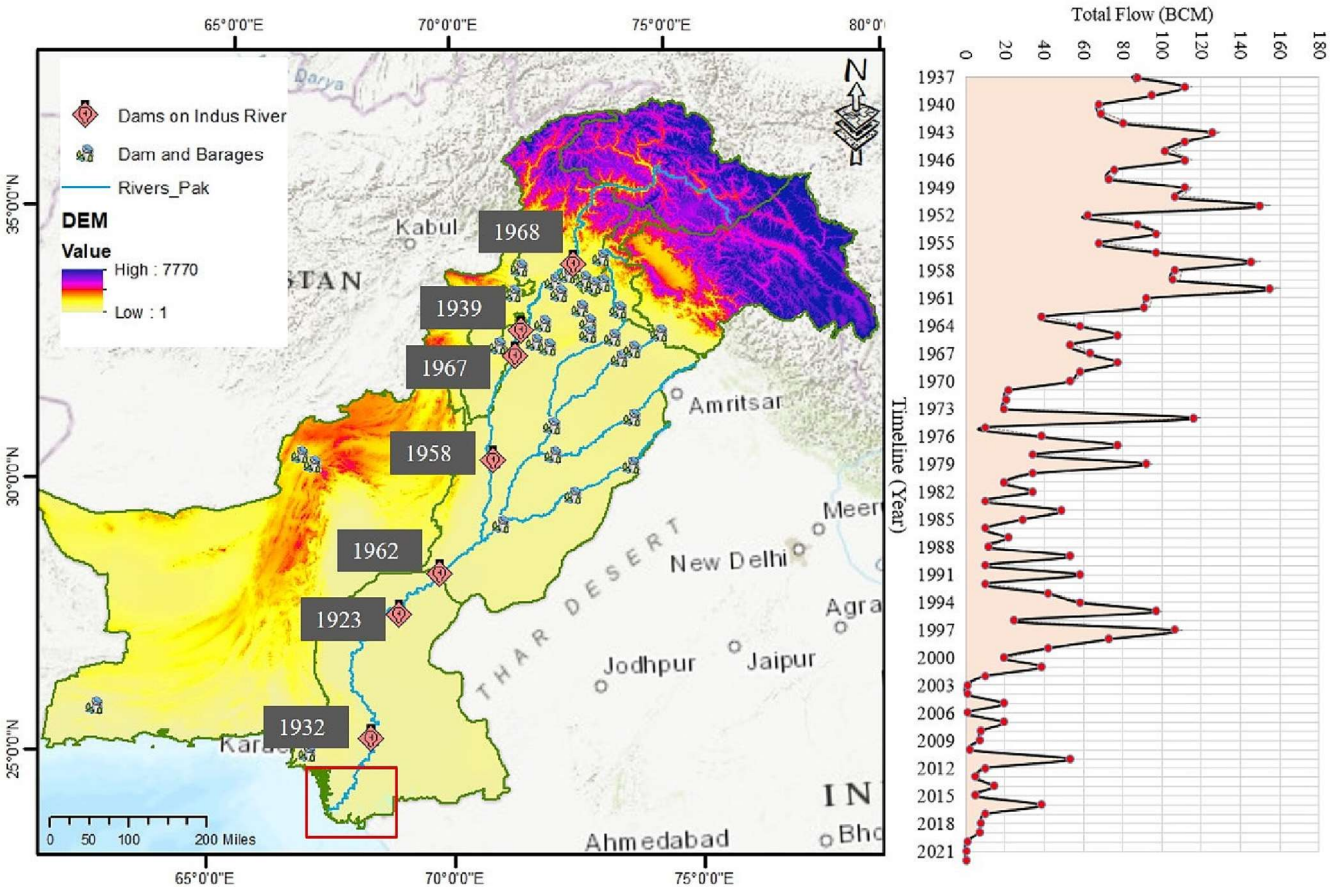

Fig. 12. Dams and barrages locations along with river flow below Kotri barrage to Indus Delta (Data source: Sindh Irrigation Department, Pakistan; Basemap Credits: Esri, Garmin, OpenStreetMap contributors, National Geographic, USGS).

2010, 2015, and 2020. The degraded mangrove sites are now converted into relatively sparse mudflats areas (i.e., not sustainable) due to rising salinity. The change detection map with black rectangles demarcates the area of mangrove loss in the corresponding region.

Previous approaches also demarcate the sites with suitable mangrove plantations and now the growth is monitored by mean of Fixed Point Photography where the smooth surface has converted into a dense thicker mangrove area in the last ten years (Bunting et al., 2018; Gilani et al., 2021) evaluating mangrove conservation and sustainability through spatiotemporal (1990–2020) mangrove cover change analysis in Pakistan. The change detection map with black rectangles demarcates the area of mangrove gain in the corresponding region. Previous approaches also demarcate these sites with mangrove plantations and now the growth is monitored using FPP where the smooth surface has converted into a dense thicker mangrove area. Several studies e.g. (Bunting et al., 2018; Gilani et al., 2021) have evaluated mangrove conservation and sustainability using spatiotemporal (1990–2020) mangrove cover change analysis for the past decade in Pakistan.

The results of this study, along with other remote sensing and machine learning techniques (Ayadi et al., 2016), bring further addition to the knowledge base on changes in mangrove cover and shoreline in different zones of the Indus Delta along the coast of Pakistan. The results indicate that the Delta is experiencing massive seawater intrusion, particularly in the mainstream area, which is affecting the growth of mangroves and water quality. The West Delta coastline assessment was categorized as a highly risked area towards erosion, and the Phitii creek area showed the highest erosion rate leading to saltwater intrusion, and a loss of mangrove cover also reported by (Dasgupta et al., 2018), highlighting the vulnerability of mangrove ecosystems in the Indus Delta. In a study conducted by (Din Hashmi and Ahmad, 2018), the salinity levels in the delta have been increasing due to various factors such as coastal intrusion and the decrease in upstream river discharge which was also found for the West and Middle West Delta (Zone II & Zone III) in this study with significant variations in salinity growth, which were mainly influenced by a decrease in upstream river discharge. Another study also reported a significant increase in salinity in the delta, with some areas reaching up to 1.83 Salinity Index value (Ijaz et al., 2019). The phenomenon of coastal erosion and mangroves is common in numerous coastal regions worldwide. For example, one such region is the Sundarbans delta, located in Bangladesh and India (Mukhopadhyay et al., 2020). In some cases, the presence of mangroves helped to mitigate coastal erosion by trapping sediment and slowing down the speed of waves (Alongi, 2015). In West Africa, mangrove forests have been cleared for commercial activities, leading to significant coastal erosion (Abuchahla et al., 2020). An example of this can be seen in the Gulf of Fonseca in Honduras, where mangroves have been used as a natural barrier to protect coastal communities from erosion (Lopez-Portillo et al., 2016).

Our study also identified areas where mangrove cover has significantly increased, such as in the NWK zone. Several studies have also highlighted the positive trend of mangroves in the Indus Delta. (Giri et al., 2014; Qureshi et al., 2019) both reported significant increases in mangrove cover in the Delta, with a 29.5 % increase observed from 1990 to 2016.

3.6. Impact on local coastal community's migration

The project villages are located on low-lying mudflats interspersed with narrow and meandering sea channels. With the decline in sediment flows downstream from Kotri barrage, the region has become highly affected by sea intrusion and land erosion. The effect is intensified because the sediments of the Indus River are retained in the dams and reservoirs upstream

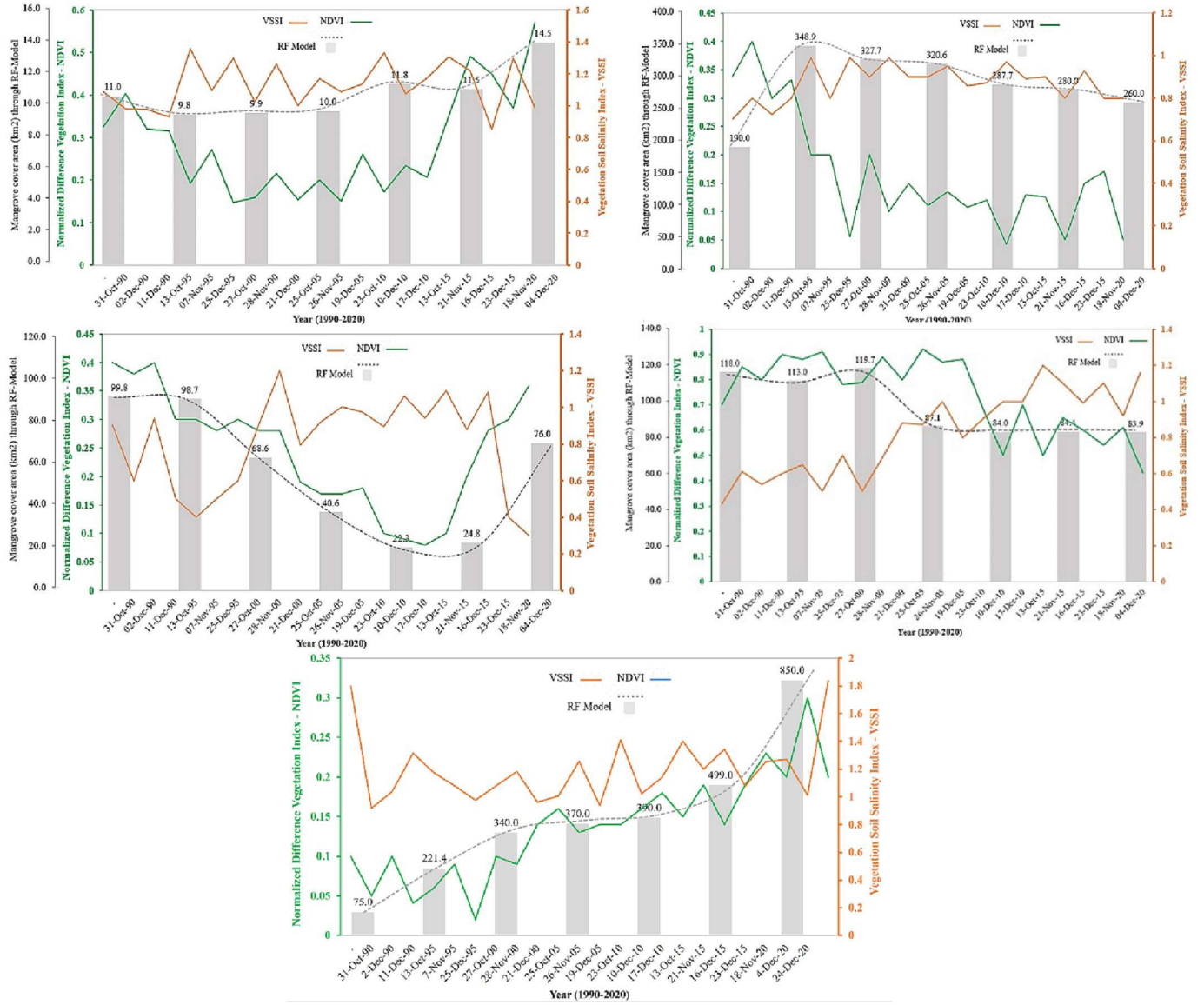

Fig. 13. Relationship between the impact of coastal saltwater intrusion on Salinity and mangrove sustainability in lower Delta using VSSI and RF; (a) NWK; (b) WD; (c) MWD; (d) MED; (e) ED.

and do not reach the delta. Most of the households have already left the project villages due to sea intrusion, land erosion, loss of agricultural land, and lack of other necessities as shown in Table 4. The participants of focus group discussions in the lower delta argued that the sea has come closer to their houses and sometimes when the wind blows, the seawater comes out to the houses. Due to sea intrusion, cultivable lands on small patches, houses, and marginal grazing lands along the coast were lost exacerbating risks and vulnerabilities. The lost lands also include healthy mangrove forests, which reduced the stock of fuelwood that local communities rely on and reduced the ability of mangrove forests, which in turn negatively affect coastal communities' livelihood.

3.7. Proposed management framework for the integrated coastal zone management in the delta

Climate Vulnerability Risk management, adaptation and mitigation plans that incorporate coastal zone management are critical aspects for addressing the challenges to the Indus Delta. Those plans should be aligned with the country's commitment to addressing climate change as part of the Nationally Determined Contributions (NDCs), National and Provincial Climate Change policies and action plans. As the level of vulnerability varies between the sites of the Delta, the Local Adaptation Plan of Action (LAPAs) at the district level are an important aspect of the in-depth planning and managing of coastal climate vulnerabilities and their associated ecosystem. Furthermore, enhanced coastal management planning is increasingly adopting a proactive and forward-thinking approach towards the sustainability of our deltaic systems. Countries such as Netherlands and UK are developing shoreline management plans that look to the 100-year timescale (Mahendra et al., 2011; Morzaria-Luna et al., 2014; Srinivasalu et al., 2009). This study's methodology offers the potential for a more sustainable and resilient future for coastal communities worldwide by departing from reactive management approaches. The Intergovernmental Panel on Climate Change (IPCC) has put forward three strategies to help combat coastal erosion: protect, accommodate, and restore. These strategies align perfectly with the Integrated Coastal Zone Management Plan (ICZMP), as previously highlighted in other studies (Ullah et al., 2021; Waldmüller et al., 2019). Moreover, to mitigate risks to the environment and human populations in Zone III and Zone IV Middle West and East Delta, we recommend the use of non-engineered solutions such as building-with-nature

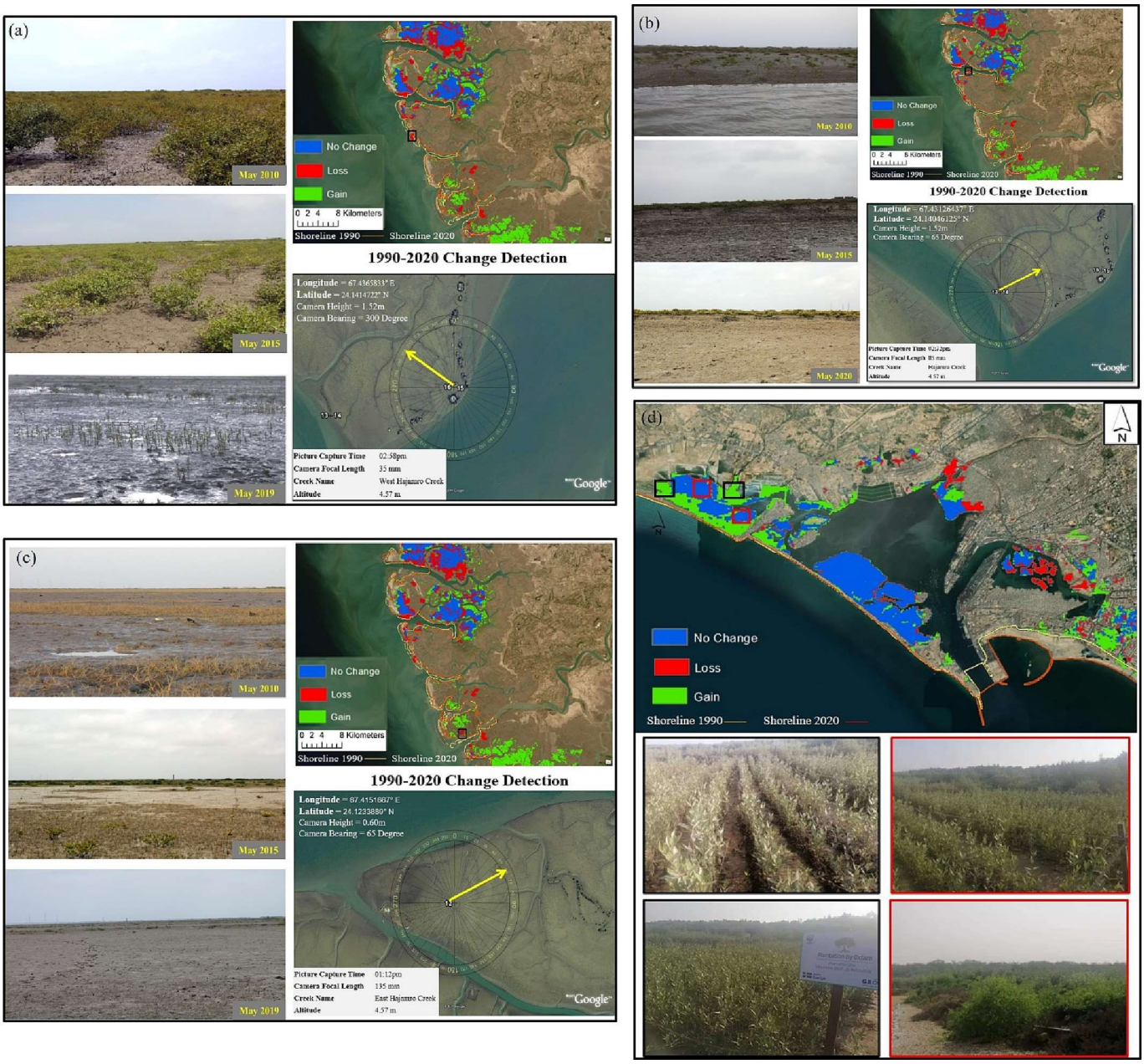

Fig. 14. Mangrove Degradation at Middle West Delta near East Hajamro Creek (black rectangle shows the area with mangroves loss and the location of photographs); (a) Hajamro creek (67.431266° E; 24.1404688° N); (b) West Hajamro creek (66.476583°E; 24.1212730°N; (c) East Hajamro creek (67.4151667° E; 24.1233889° N); (d) Sandspit creek (66.57213°E; 24.511834°N).

Table 4
Villages and household migration from the most vulnerable creeks due to coastal intrusion.

Villages migrated to	Migrated villages	Migrated household (HH)	Migrated village	Migrated household (HH)
Meero	Tippan	230	Meero Dablo	232
	Kharyoon	200	Hassan	194
Yousaf Katiyar	Mamo Shedi	74	Gilli	194
	Mamo Dablo	157	Sholani	65
Urban	Mamo Shedi	74	Ismail	226
	Mamo Dablo	157	Yousaf	711
	Gilli	194	Khtiyar	464
	Cheer	65		

practices, including the cultivation of salt-tolerant mangroves. This approach can help to combat coastal recession and promote long-term coastal sustainability in the study area (van Slobbe et al., 2013). To stabilize the coastline, it is essential to restore the mangroves that have been lost and conserve the remaining ones (Mukhtar and Hannan, 2012). These soft techniques offer flexibility, are reversible, and allow for a wide range of shoreline management plans. By supplementing natural processes, coastal communities can adapt to changing requirements and safeguard their environment sustainably. To accommodate coastal erosion, vulnerable areas can be retained with current land use and restored near-shore delta. However, new constructions of dams and barrages upstream of the Indus River should be avoided to prevent a reduction in sediment deposition in the Indus Delta. Moreover, effective solutions are possible within an integrated coastal management framework, but there may be barriers to implementation. Technical support and stakeholder engagement can help overcome these challenges and choose the best management strategy. ICZM can

serve as a platform for co-creation and education of stakeholders on available adaptation options.

4. Conclusion

To evaluate the shrinking shoreline of the Indus delta over the past thirty years, this study utilized an integrated multispectral statistical approach. The study identifies that the primary causes of erosion include the reduced sediment deposition resulting from water infrastructure development and climate change. The tasselled cap transformation analysis was employed to calculate coastal erosion and accretion at various zones, through the linear regression rates approach. The study identified the Northwest and Western Delta segments as highly erosional, which is crucial in the context of coastal communities and important for effective coastal planning, appropriate actions, and adaptation measures to mitigate erosion processes for coastal sustainability, particularly in highly vulnerable regions. The work suggests that in the absence of effective and immediate measures, the coastline erosion trend will persists and continue to impact the eastern region.

The relevant authorities at federal and provincial level should therefore prioritize research and action-plans for preventing, mitigating measures, in high erosion areas, which are home to thousands of migratory birds and a source of livelihood for millions. The results of this work could serve as a roadmap for identifying regions with higher coastal erosion, enabling further in-depth assessments to reduce erosion and associated risks in Pakistan.

The findings of this research can significalty contribute for formulation of policies and management planning of coastal resources and addressing vulnerabilities of coastal communities. Evidence generated through this work would also support in leveraging from opportunities the newly established climate change loss and damage fund establishments to address the costs of extreme weather events and other climate-related impacts that go beyond adaptation, should be considered a priority to secure the vulnerable sites. It also aims to support adaptation, mitigation, and other measures to reduce the risk and impact of climate change on vulnerable countries and communities. It is also recommended that the emerging and green solutions such as Nature-based solutions (NbS) which integrate green infrastructures, mangrove restoration, wetland conservation and restoration measures and their long-term monitoring offer sustainable could offer sustainable solutions to address the challenges faced by sinking Indus Delta. While the current study offers valuable and credible insights on the state of changes and vulnerability of the Indus Delta, it can benefit greatly from field verifications to help to overcome uncertainties especially for long-term research and monitoring.

CRediT authorship contribution statement

Hafsa Aeman: Conceptualization, Data Collection, Analysis, Writing. Hong Shu: Conceptualization, Supervising. Sawaid Abbas: Visualization, Analysis, Writing - review and editing, Hamera Aisha: Data Collection, Validation, editing. Muhammad Usman: Editing – Revision.

Data availability

Data will be made available on request.

Declaration of competing interest

The authors declare that they have no known competing financial interests or personal relationships that could have appeared to influence the work reported in this paper.

Acknowledgements

We are delighted to acknowledge the State Key Laboratory of Information Engineering in Surveying, Mapping and Remote Sensing, Wuhan University, China for providing a social, speculative, and educational framework to facilitate and nurture research of this magnitude. We want to acknowledge Prof. Hong Shu, and Lab mates from the LIESMARS lab, Saeed-ul-Islam from WWF-Pakistan for their support and guidance during this research and all the organization names used in this research for helping to obtain the ground truth data.

Appendix A. Supplementary data

Supplementary data to this article can be found online at https://doi.org/10.1016/j.scitotenv.2023.163356.

References

Abbas, S., Qamer, F.M., Ali, G., Tripathi, N.K., Shehzad, K., Saleem, R., Gilani, H., 2013. An assessment of status and distribution of mangrove forest cover in Pakistan. 3, 64–78.

Abbas, S., Qamer, F.M., Hussain, N., Saleem, R., Nitin, K.T., 2012. National Level Assessment of mangrove Forest cover in Pakistan. Int. Arch. Photogramm. Remote. Sens. Spat. Inf. Sci. XXXVIII-8/, 187–192. https://doi.org/10.5194/isprsarchives-xxxviii-8-w20-187-2011.

Abuchahla, G.M., Olajuyigbe, S., Abuchahla, J.C., 2020. Human and natural factors of mangrove loss and the implications on coastal erosion in West Africa. J. Afr. Earth Sci. 170, 103966.

Adarsa, J., Shamina, S., Arkoprovo, B., 2012. Morphological change study of Ghoramara Island, eastern India using multi temporal satellite data. Res. J. Recent Sci. 1 (10), 72–81.

Ahmed, I., Ahmed, N., Ullah, S., Hussain, M., 2021. Spatial and temporal variations of mangrove cover in the Indus Delta during 1990–2016 using Landsat satellite data. Environ. Monit. Assess. 193 (2), 1–17. https://doi.org/10.1007/s10661-021-09164-9.

Alhammadi, M.S., Glenn, E.P., 2008. Detecting date palm trees health and vegetation greenness change on the eastern coast of the United Arab Emirates using SAVI. Int. J. Remote Sens. 29 (6), 1745–1765. https://doi.org/10.1080/01431160701395195.

Alongi, D.M., 2015. The impact of climate change on mangrove forests. Curr. Clim. Change Rep. 1 (1), 30–39.

Amjad, A.S., Kasawani, I., Kamaruzaman, J., 2007. Degradation of Indus Delta mangroves in Pakistan. Int. J. Geol. 1 (3), 27–34.

Ayadi, K., Boutiba, M., Sabatier, F., Guettouche, M.S., 2016. Detection and analysis of historical variations in the shoreline, using digital aerial photos, satellite images, and topographic surveys DGPS: case of the Bejaia bay (East Algeria). Arab. J. Geosci. 9 (3), 198. https://doi.org/10.1007/s12517-015-2043-9.

Baig, M.R.I., Ahmad, I.A., Shahfahad, Tayyab, M., Rahman, A., 2020. Analysis of shoreline changes in Vishakhapatnam coastal tract of Andhra Pradesh, India: an application of digital shoreline analysis system (DSAS). Annals of GIS 26 (3), 183–193. https://doi.org/10.1080/19475683.2020.1815839.

Bunting, P., Rosenqvist, A., Lucas, R., Rebelo, L.-M., Hilarides, L., Thomas, N., Hardy, A., Itoh, T., Shimada, M., Finlayson, C., 2018. The global mangrove Watch—A new 2010 global baseline of mangrove extent. Remote Sens. 10 (10), 1669. https://doi.org/10.3390/rs10101669.

Crist, E.P., 1985. A TM tasseled cap equivalent transformation for reflectance factor data. Remote Sens. Environ. 17 (3), 301–306. https://doi.org/10.1016/0034-4257(85)90102-6.

Cui, B.L., Li, X.Y., 2011. Coastline change of the Yellow River estuary and its response to the sediment and runoff (1976–2005). Geomorphology 125 (1), 184–195. https://doi.org/10.1016/j.geomorph.2010.12.00.

Dasgupta, R., Qamer, F.M., Rafique, M., 2018. Vanishing mangroves in the indus delta: implications for the sustainability of the Indus water treaty. Int. J. Water Resour. Dev. 34 (5), 691–703.

Dehni, A., Lounis, M., 2012. Remote sensing techniques for salt affected soil mapping: application to the Oran region of Algeria. Procedia Eng. 33, 188–198. https://doi.org/10.1016/j.proeng.2012.01.1193.

Din Hashmi, S.G.M., Ahmad, S.R., 2018. GIS-based analysis and modeling of coastline erosion and accretion along the coast of Sindh Pakistan. Coast. Zone Manag. J. 21 (6), 455. https://doi.org/10.4172/2473-3350.1000455.

Douaoui, A.E.K., Nicolas, H., Walter, C., 2006. Detecting salinity hazards within a semiarid context by means of combining soil and remote-sensing data. Geoderma 134 (1–2), 217–230. https://doi.org/10.1016/j.geoderma.2005.10.009.

DSAS, 2005. Digital Shoreline Analysis System (Version 4.4) [Software]. . https://woodshole.er.usgs.gov/project-pages/DSAS/.

Durduran, S.S., 2010. Coastline change assessment on water reservoirs located in the Konya Basin area, Turkey, using multitemporal Landsat imagery. Environ. Monit. Assess. 166 (1–4), 339–350. https://doi.org/10.1007/s10661-009-0906-9.

Eisavi, V., Homayouni, S., Yazdi, A.M., Alimohammadi, A., 2015. Land cover mapping based on random forest classification of multitemporal spectral and thermal images. Environ. Monit. Assess. 187, 1–14.

Gao, B.C., 1996. NDWI—A normalized difference water index for remote sensing of vegetation liquid water from space. Remote sensing of environment 58 (3), 257–266.

Genz, A.S., Fletcher, C.H., Dunn, R.A., Frazer, L.N., Rooney, J.J., 2007. The predictive accuracy of shoreline change rate methods and alongshore beach variation on MauiHawaii. Journal of Coastal Research 23, 932–949. https://doi.org/10.2112/05-0521.1.

Ghosh, M.K., Kumar, L., Roy, C., 2015. Monitoring the coastline change of Hatiya Island in Bangladesh using remote sensing techniques. ISPRS J. Photogramm. Remote Sens. 101, 137–144.

Gilani, H., Naz, H.I., Arshad, M., Nazim, K., Akram, U., Abrar, A., Asif, M., 2021. Evaluating mangrove conservation and sustainability through spatiotemporal (1990–2020) mangrove cover change analysis in Pakistan. Estuar. Coast. Shelf Sci. 252, 107128. https://doi.org/10.1016/j.ecss.2020.107128.

Giosan, L., Constantinescu, S., Clift, P.D., Tabrez, A.R., Danish, M., Inam, A., 2006. Recent morphodynamics of the indus delta shore and shelf. Cont. Shelf Res. 26 (14), 1668–1684.
Giri, C., Long, J., Abbas, S., Murali, R.M., Qamer, F.M., Pengra, B., Thau, D., 2014. Distribution and dynamics of mangrove forests of South Asia. J. Environ. Manag. 1–11. https://doi.org/10.1016/j.jenvman.2014.01.020.
Giri, C., Ochieng, E., Tieszen, L.L., Zhu, Z., Singh, A., Loveland, T., Duke, N., 2011. Status and distribution of mangrove forests of the world using earth observation satellite data. Glob. Ecol. Biogeogr. 20 (1), 154–159.
Goldsmid, F.J., Haig, M.R., 1895. The Indus-Delta country. Review. The Geographical Journal 6 (3), 260. https://doi.org/10.2307/1774251.
Ijaz, M.W., Mahar, R.B., Ansari, K., Siyal, A.A., 2019. Optimization of salinity intrusion control through freshwater and tidal inlet modifications for the Indus River estuary. Estuar. Coast. Shelf Sci. 224, 172–182. https://doi.org/10.1016/j.ecss.2019.04.039.
Ji, H., Pan, S., Chen, S., 2020. Impact of river discharge on hydrodynamics and sedimentary processes at Yellow River Delta. Mar. Geol. 425, 106210.
Kalivas, D.P., Kollias, V.J., Karantounias, G., 2003. A GIS for the assessment of the spatio-temporal changes of the Kotychi lagoon, Western Peloponnese, Greece. Water Resour. Manag. 17, 19–36.
Kanwal, S., Ding, X., Sajjad, M., Abbas, S., 2019. Three decades of coastal changes in Sindh, Pakistan (1989–2018): a geospatial assessment. Remote Sens. 12 (1), 8.
Khan, N.M., Rastoskuev, V.V., Sato, Y., Shiozawa, S., 2005. Assessment of hydrosaline land degradation by using a simple approach of remote sensing indicators. Agric. Water Manag. 77 (1–3), 96–109.
Kuleli, T., Guneroglu, A., Karsli, F., Dihkan, M., 2011. Automatic detection of shoreline change on coastal Ramsar wetlands of Turkey. Ocean Eng. 38 (10), 1141–1149.
Li, X., Chen, D., Duan, Y., Ji, H., Zhang, L., Chai, Q., Hu, X., 2020. Understanding land use/Land cover dynamics and impacts of human activities in the Mekong Delta over the last 40 years. Glob. Ecol. Conserv. 22, e00991.
Liou, Y.A., Nguyen, A.K., Li, M.H., 2017. Assessing spatiotemporal eco-environmental vulnerability by Landsat data. Ecol. Indic. 80, 52–65.
Lira, C., Taborda, R., 2014. Advances in applied remote sensing to coastal environments using free satellite imagery. RemoteSensing and Modeling: Advances in Coastal and Marine Resources, pp. 77–102.
Liu, Y., Huang, H., Qiu, Z., Chen, J., Yang, X., 2012. Monitoring change and position of coastlines from satellite images using slope correction in a tidal flat: a case study in the yellow river delta. Acta Geogr. Sin 67 (3), 377–387.
Lopez-Portillo, J., Ezcurra, E., Ramirez-Ortiz, J., 2016. Mangrove forests as natural bio-shields against hurricanes and storms. Front. Ecol. Environ. 14 (7), 352–353.
Mahboob, M.A., Atif, I., 2016. Coastline change detection using moderate resolution satellite imagery: a case study of makran coast, Arabian SeaPakistan. Science International 28 (1), 273–277.
Mahendra, R.S., Mohanty, P.C., Bisoyi, H., Kumar, T.S., Nayak, S., 2011. Assessment and management of coastal multi-hazard vulnerability along the Cuddalore-villupuram, east coast of India using geospatial techniques. Ocean Coast. Manag. 54 (4), 302–311.
Mallah, H.B., 2013. Social inequality and environmental threats in Indus Delta Villages: Pakistan. ESF-UniBI-ZIF Research Conference on 'Tracing Social Inequalities in Environmentally-induced Migration. 118, p. 28.
Morzaria-Luna, H.N., Castillo-López, A., Danemann, G.D., Turk-Boyer, P., 2014. Conservation strategies for coastal wetlands in the Gulf of CaliforniaMexico. Wetlands Ecology and Management 22 (3), 267–288. https://doi.org/10.1007/s11273-013-9328-0.
Mukhopadhyay, A., Bhadra, B., Rakshit, D., 2020. Coastal erosion in the Sundarbans delta: causes, consequences and management. Mar. Pollut. Bull. 154, 111082.
Mukhtar, I., Hannan, A., 2012. Constrains on mangrove forests and conservation projects in Pakistan. J. Coast. Conserv. 16, 51–62.
Nasir, S.M., Akbar, G., 2012. Effect of river indus flow on low riparian ecosystems of Sindh: a review paper. Rec. Zool. Surv. Pakistan 21, 86–89.
Nassar, K., Mahmod, W.E., Fath, H., Masria, A., Nadaoka, K., Negm, A., 2019. Shoreline change detection using DSAS technique: case of North Sinai coastEgypt. Marine Georesources & Geotechnology 37 (1), 81–95.
Parizi, E., Hosseini, S.M., Ataie-Ashtiani, B., Simmons, C.T., 2019. Vulnerability mapping ofcoastal aquifers to seawater intrusion: review, development and application. J. Hydrol. 570, 555–573. https://doi.org/10.1016/j.jhydrol.2018.12.021.
Passer, D.L., Hagent, S.C., Irish, J.L., 2014. Comparison of shoreline change rates along the South Atlantic bight and northern Gulf of Mexico coasts for better evaluation of future shoreline positions under sea level rise. J. Coast. Res. 68, 20–26. https://doi.org/10.2112/si68-003.1.
Petropoulos, G.P., Kalivas, D.P., Griffiths, H.M., Dimou, P.P., 2015. Remote sensing and GIS analysis for mapping spatio-temporal changes of erosion and deposition of two Mediterranean river deltas: the case of the axios and aliakmonas rivers, Greece. Int. J. Appl. Earth Obs. Geoinf. 35, 217–228.
Pimple, U., Simonetti, D., Sitthi, A., Pungkul, S., Leadprathom, K., Skupek, H., Som-ard, J., Gond, V., Towprayoon, S., 2018. Google earth engine based three decadal landsat imagery analysis for mapping of mangrove forests and its surroundings in the Trat Province of Thailand. J. Comput. Commun. 6 (1), 247–264. https://doi.org/10.4236/jcc.2018.61025.
Qureshi, M.A., Hussain, I., Ali, K., Ali, M., 2019. Spatiotemporal dynamics of mangrove forest using remote sensing and GIS techniques in the Indus DeltaPakistan. Environmental monitoring and assessment 191 (5), 299.
Saavedra, C., 2005. Estimating spatial patterns of soil erosion and deposition in the Andean region using geo-information techniques Acase study in Cochabamba, Bolivia. ITC Dissertation CN - S625.B5 S33 2005.
Sanderman, J., Hengl, T., Fiske, G., Solvik, K., Adame, M.F., Benson, L., Landis, E., 2018. A global map of mangrove forest soil carbon at 30 m spatial resolution. Environ. Res. Lett. 13 (5), 055002.
Sarwar, M.G.M., Woodroffe, C.D., 2013. Rates of shoreline change along the coast of Bangladesh. J. Coast. Conserv. 17, 515–526.
Semenov, S.M., Abushenko, N.A., Chichigin, A.S., 1999. Discrimination of shorelines on satellite images from boundary-point and halftone information. Mapp. Sci. Remote. Sens. 36 (4), 245–255.
Shi, T., Liu, J., Hu, Z., Liu, H., Wang, J., Wu, G., 2016. New spectral metrics for mangrove forest identification. Remote Sens. Lett. 7 (9), 885–894.
Siddiqui, M.N., Maajid, S., 2004. Monitoring of geomorphological changes for planning reclamation work in coastal area of KarachiPakistan. Advances in Space Research 33 (7), 1200–1205.
Solangi, G.S., Siyal, A.A., Siyal, P., 2023. Indication of subsurface seawater intrusion into the Indus delta, Sindh, Pakistan. Mehran Univ. Res. J. Eng. Technol. 42 (1), 9. https://doi.org/10.22581/muet1982.2301.02.
Solangi, G.S., Siyal, A.A., Babar, M.M., Siyal, P., 2020. Temporal dynamics of vegetative cover and surface water bodies in the Indus delta, Pakistan. Mehran Univ. Res. J. Eng. Technol. 39 (1), 133–144.
Solangi, K.A., Siyal, A.A., Wu, Y., Abbasi, B., Solangi, F., Lakhiar, I.A., Zhou, G., 2019. An assessment of the spatial and temporal distribution of soil salinity in combination with field and satellite data: a case study in Sujawal District. Agronomy 9 (12), 869.
Srinivasalu, S., Rajeshwara Rao, N., Thangadurai, N., Jonathan, M.P., Roy, P.D., Ram Mohan, V., Saravanan, P., 2009. Characteristics of 2004 tsunami deposits of the northern Tamil Nadu coast, southeastern India. Bol. Soc. Geol. Mex. 61 (1), 111–118. https://doi.org/10.18268/BSGM2009v61n1a10.
Suresh, P.K., Sundar, V., 2011. Prediction of "shore line evolution andestimation of littoral drift at the tip of Indian peninsula". J. Hydro environment research 5, 157–167.
Ullah, Z., Wu, W., Wang, X.H., Pavase, T.R., Shah, S.B.H., Pervez, R., 2021. Implementation of a marine spatial planning approach in Pakistan: an analysis of the benefits of an integrated approach to coastal and marine management. Ocean Coast. Manag. 205, 105545.
van Slobbe, E., de Vriend, H.J., Aarninkhof, S., Lulofs, K., de Vries, M., Dircke, P., 2013. Building with nature: in search of resilient storm surge protection strategies. Nat. Hazards 66 (3), 1461–1480. https://doi.org/10.1007/s11069-013-0612-3.
Verma, K.S., Saxena, R.K., Barthwal, A.K., Deshmukh, S.N., 1994. Remote sensing technique for mapping salt affected soils. Int. J. Remote Sens. 15 (9), 1901–1914.
Waldmüller, J.M., Jamali, H., Nogales, N., 2019. Operationalizing sustainable development goals in vulnerable coastal areas of Ecuador and Pakistan: marginalizing human development? J. Hum. Dev. Capab. 20 (4), 468–485. https://doi.org/10.1080/19452829.2019.1666810.
Waqas, M., Nazeer, M., Shahzad, M.I., Zia, I., 2019. Spatial and temporal variability of open-ocean barrier islands along the Indus Delta region. Remote Sens. 11 (4), 437.
WWF-Pakistan, 2005. GIS remote sensing based assessment of mangrove resources of selected project sites of Indus Delta and Makran coast. 55.
Zeferino, L.B., de Souza, L.F.T., do Amaral, C.H., Fernandes Filho, E.I., de Oliveira, T.S., 2020. Does environmental data increase the accuracy of land use and land cover classification? International Journal of Applied Earth Observation and Geoinformation 91, 102128.
Zhang, Y., Li, X., Zhang, J., Song, D., 2013. . JanuaryAbstract and Applied Analysis 2013 Hindawi.
Zhao, Y., Potgieter, A.B., Zhang, M., Wu, B., Hammer, G.L., 2020. Predicting wheat yield at the field scale by combining high-resolution Sentinel-2 satellite imagery and crop modelling. Remote Sens. 12 (6), 1024.
Zhu, Q., Li, P., Li, Z., Pu, S., Wu, X., Bi, N., Wang, H., 2021. Spatiotemporal changes of coastline over the Yellow River Delta in the previous 40 years with optical and SAR remote sensing. Remote Sens. 13 (10), 1940.